MÁSTER UNIVERSITARIO EN INGENIERÍA INDUSTRIAL

TRABAJO FIN DE MÁSTER

3D BLADE MODEL UPDATING BY COUPLING HAWC2 AND ABAQUS

Autor: María Luz Castilla Mena

Director: Xiao Chen

Madrid

Junio de 2023

Declaro, bajo mi responsabilidad, que el Proyecto presentado con el título 3D BLADE MODEL UPDATING BY COUPLING HAWC2 AND ABAQUS en la ETS de Ingeniería - ICAI de la Universidad Pontificia Comillas en el curso académico 2022-2023 es de mi autoría, original e inédito y no ha sido presentado con anterioridad a otros efectos. El Proyecto no es plagio de otro, ni total ni parcialmente y la información que ha sido tomada de otros documentos está debidamente referenciada.

Fdo.: María Luz Castilla Mena Fecha: 13/ 03/2023

Autorizada la entrega del proyecto

EL DIRECTOR DEL PROYECTO

Fdo.: Xiao Chen Fecha: 13/03/2023

MÁSTER UNIVERSITARIO EN INGENIERÍA INDUSTRIAL

TRABAJO FIN DE MÁSTER

3D BLADE MODEL UPDATING BY COUPLING HAWC2 AND ABAQUS

Autor: María Luz Castilla Mena

Director: Xiao Chen

Madrid

Junio de 2023

ACTUALIZACION DEL MODELO 3D DE UNA PALA EOLICA MEDIANTE EL ACOPLAMIENTO DE HAWC2 Y ABAQUS

Autor: Castilla Mena, María Luz.

Director: Chen, Xiao.

Entidad Colaboradora: Universidad Técnica de Dinamarca (DTU).

RESUMEN DEL PROYECTO

Introducción

Planteamiento del Problema

En la actualidad, vivimos en un mundo en el que la demanda de energía está aumentando y existe una gran preocupación por obtener energía limpia a partir de fuentes renovables. La energía eólica se ha convertido en un elemento fundamental de la red eléctrica, y cada vez se construyen más aerogeneradores en zonas costeras donde hay una gran demanda de energía y un amplio recurso eólico. Como consecuencia, las turbinas eólicas están más expuestas a condiciones de vientos fuertes, como tifones y huracanes, que suponen un peligro importante para su integridad estructural. La Figura 1, extraída de la referencia [1], muestra cómo un tornado pone al límite la respuesta estructural de una pala de un aerogenerador. El tornado tuvo lugar en Crowell, Texas, el 4 de mayo de 2022. Es evidente lo mucho que puede doblarse una pala de un aerogenerador con estos fuertes vientos debido a las importantes desviaciones que experimenta, y pueden inducirse daños en la pala en estas condiciones. Sin embargo, las condiciones meteorológicas extremas no sólo afectan a los aerogeneradores marinos, sino también a los terrestres.

Figure 1: Desviación de las palas de un aerogenerador bajo la influencia de una tormenta. Figura extraída de la referencia [1].

Como las turbinas eólicas están expuestas a condiciones externas, es inevitable que su rendimiento se deteriore con el tiempo. Es importante saber que, en el contexto aeroelástico de un aerogenerador, tanto las cargas aerodinámicas como las propiedades estructurales se influyen mutuamente. Las cargas aerodinámicas pueden hacer que la pala se deforme y estas deformaciones cambian la dirección del flujo del viento, modificando las cargas aerodinámicas. Esto es lo que se denomina un problema acoplado.

En condiciones de viento extremas como las que muestra la Figura 1, los aerogeneradores se ven expuestos a una situación fuera de sus límites de diseño en la que se desconoce cómo puede evolucionar su estado. Pueden inducirse daños en la estructura de las palas y degradarse las propiedades de rigidez debido a las cargas aerodinámicas extremas. Si no se sustituyen a tiempo, podrían dañar toda la estructura del aerogenerador.

Estado del Arte

Las herramientas aeroelásticas se utilizan para calcular la respuesta temporal de un aerogenerador en determinadas condiciones de viento, calculando las cargas aerodinámicas de forma fácil y sencilla. El procedimiento seguido por las herramientas aeroelásticas consiste en dividir la estructura de la pala del aerogenerador en secciones, modelando cada sección como un elemento viga (véase la Figura 2). La herramienta aeroelástica considera cada sección de la pala como una única línea, sin altura ni anchura, y con propiedades de rigidez constantes. Con este enfoque, no se tienen en cuenta las no-linealidades asociadas a la geometría, el material o la composición del compuesto.

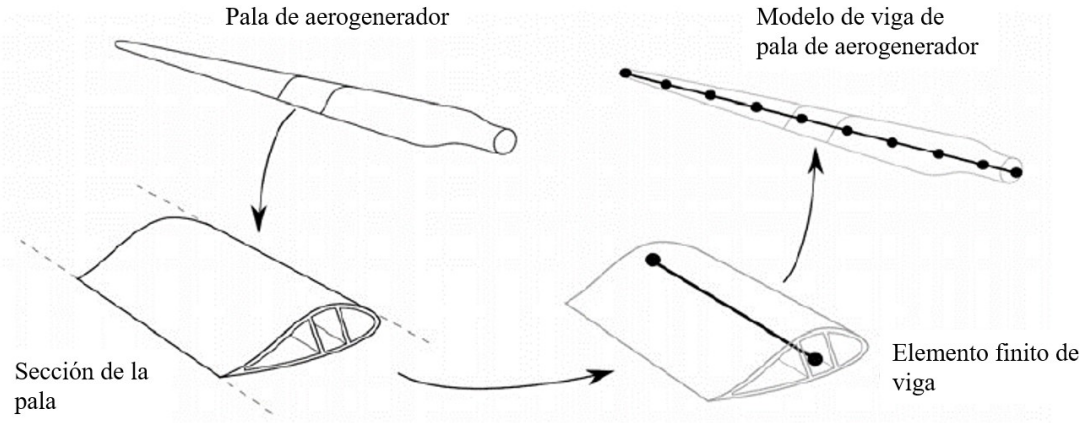

Figure 2: Enfoque por elementos de viga. Figura tomada de la referencia [2].

Sin embargo, en condiciones meteorológicas extremas en las que pueden inducirse daños en la estructura de las palas, este enfoque basado en elementos viga no tiene en cuenta la degradación estructural. Esta hipótesis no es suficiente para calcular con precisión las cargas aerodinámicas, ya que no tiene en cuenta la geometría de la estructura, ni si hay delaminación en el material compuesto o aplastamiento del núcleo de espuma.

Objetivos del Proyecto

La idea detrás de este estudio es desarrollar una interfaz que acople la herramienta aeroelástica HAWC2 con el software 3D de elementos finitos ABAQUS para considerar la degradación de las propiedades de rigidez cuando se induce daño en una sección de pala de aerogenerador bajo condiciones extremas de viento. Con esta interfaz, se consideran las interacciones entre los sistemas aeroelásticos y estructurales.

Si en condiciones de viento extremo se producen daños en la estructura de la pala, el software 3D de elementos finitos calculará las propiedades de rigidez en una sección de pala 3D y la interfaz las actualizará en la herramienta aeroelástica HAWC2 para calcular las cargas aerodinámicas correspondientes. Siguiendo este enfoque, se pueden lograr

simulaciones precisas correspondientes a escenarios de vientos extremos, ayudando así a predecir el comportamiento del aerogenerador en condiciones de viento extremas.

Metodología de trabajo

El flujo de trabajo general de la interfaz se muestra en la Figura 3. La interfaz se desarrollará en MATLAB.

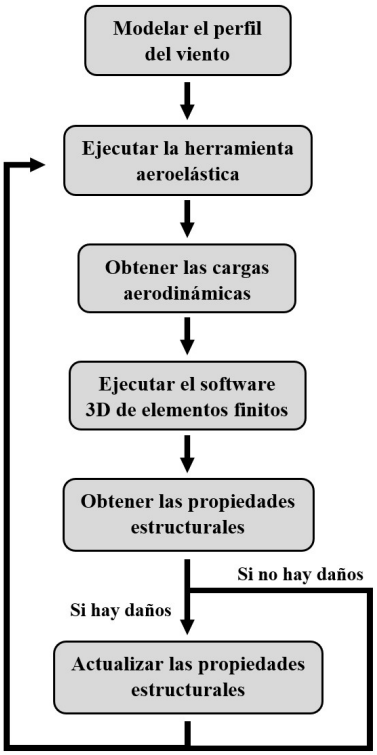

Figure 3: Flujo de trabajo general de la interfaz de MATLAB.

El flujo de trabajo general de la interfaz de MATLAB consta de los seis pasos principales siguientes.

- **Paso 1: Modelar el perfil del viento**. En primer lugar, es necesario describir el perfil de viento extremo para que pueda ser modelado por la herramienta de simulación aeroelástica y utilizarlo como dato de entrada, o input.
- **Paso 2: Ejecución de la simulación aeroelástica**. Una vez modelado el perfil de viento extremo, se ejecuta la simulación aeroelástica y se calculan las cargas aerodinámicas en las palas del aerogenerador.
- **Paso 3: Obtener las cargas aerodinámicas**. La interfaz lee los resultados obtenidos de las simulaciones aeroelásticas.
- **Paso 4: Ejecutar la simulación 3D de elementos finitos**. A continuación, se aplican las cargas aerodinámicas a la estructura 3D de la pala del aerogenerador, se ejecuta la simulación 3D de elementos finitos y se obtienen las propiedades estructurales.

- **Paso 5: Obtener las propiedades de rigidez**. La interfaz lee los resultados obtenidos de las simulaciones 3D de elementos finitos y calcula las nuevas propiedades de rigidez de las secciones de las palas del aerogenerador.
- **Si se detecta un fallo en la estructura de la pala**:
  - **Paso 6: Actualizar propiedades de rigidez**. La interfaz actualiza las propiedades de rigidez en la herramienta de simulación aeroelástica. Como resultado, las nuevas cargas aerodinámicas pueden ser calculadas de nuevo ejecutando la simulación aeroelástica.
- **Si no se encuentra ningún fallo en la estructura de la pala**. No es necesario actualizar las propiedades de rigidez y las cargas aerodinámicas pueden calcularse de nuevo ejecutando la herramienta de simulación aeroelástica.

Para ejecutar la interfaz y realizar las simulaciones, es necesario definir tanto la configuración aeroelástica como la configuración de elementos finitos en el software 3D. En el caso de la configuración aeroelástica, hay que definir las especificaciones del aerogenerador para realizar las simulaciones y modelar el perfil del viento. En el caso del software de elementos finitos 3D ABAQUS, hay que definir la sección 3D de la pala, calcular las propiedades de rigidez y realizar un análisis del fallo de la pala.

En cuanto a las especificaciones del aerogenerador para la configuración aeroelástica, se ha seleccionado el aerogenerador de referencia de DTU (de la Universidad Técnica de Dinamarca) de 10 MW como aerogenerador para este estudio. Para el diseño estructural, la pala se ha dividido en 51 secciones a lo largo de su longitud. Cada sección se ha modelado como elementos de viga con propiedades de rigidez constantes, correspondientes a su sección transversal respectiva.

Además, es necesario modelar un perfil de viento extremo, ya que el objetivo es inducir daños en la estructura de las palas. Según la escala Saffir-Simpson, los perfiles de viento con una velocidad media de alrededor de 33-43 m/s pueden producir daños en los edificios. Además, el perfil de viento debe tener una ráfaga de viento notable, ya que las tormentas se caracterizan por tener un aumento repentino de la velocidad del viento. Se eligieron mediciones de datos reales que cumplían estas características, correspondientes a un mástil en Skipheya, en la isla noruega de Froya. Sin embargo, para modelar el perfil del viento en la herramienta aeroelástica HAWC2, existen algunos requisitos. Es necesario modelar el perfil del viento a la altura del buje, y las 3 componentes del campo de viento (componentes u, v y w) son necesarias para modelar el perfil del viento. La componente u se obtiene a partir de las mediciones de datos reales, mientras que las componentes v y w se calculan utilizando un paquete de generación de campos de turbulencia. Con esta herramienta, se puede simular una caja de turbulencia restringida para recrear las estructuras de flujo. La caja de turbulencia es la herramienta utilizada para simular el perfil del viento, contiene en su interior todo el campo de turbulencia y asume que se mueve con la velocidad media del viento hacia el aerogenerador. La caja de turbulencia se genera restringiendo una única componente, que en este caso es la componente u, ya que es la que se obtiene de las medidas de turbulencia del fichero de datos. La Figura 4 muestra el aspecto de una caja de turbulencia y los parámetros necesarios para definirla.

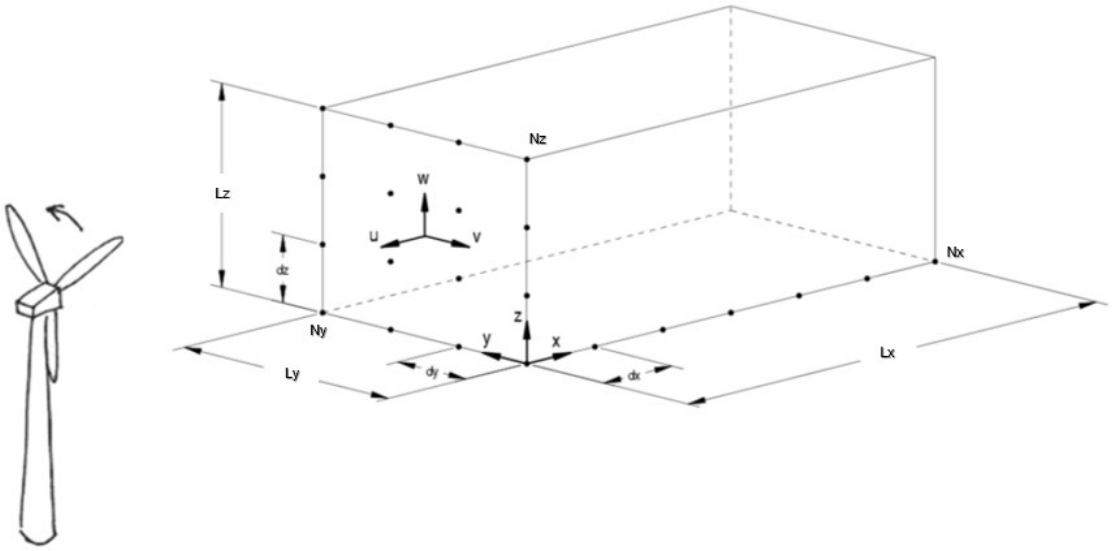

Figure 4: Dimensiones de la caja de turbulencia. Figura extraída de la referencia [3].

De acuerdo con la configuración de elementos finitos 3D, es necesario definir la sección 3D de las palas. La sección de pala 3D que se ha utilizado para este estudio se ha modelado de acuerdo con el diseño estructural del aerogenerador de referencia de 10 MW de DTU. La pala está fabricada con materiales compuestos reforzados con fibra de vidrio y estructuras sándwich con núcleo de espuma, como se muestra en la figura 5. Si se inducen daños en la sección de la pala, las propiedades de rigidez se recalcularán para la estructura de la pala con el software 3D de elementos finitos ABAQUS, y la interfaz las actualizará en la herramienta aeroelástica HAWC2 para el siguiente cálculo de las cargas aerodinámicas.

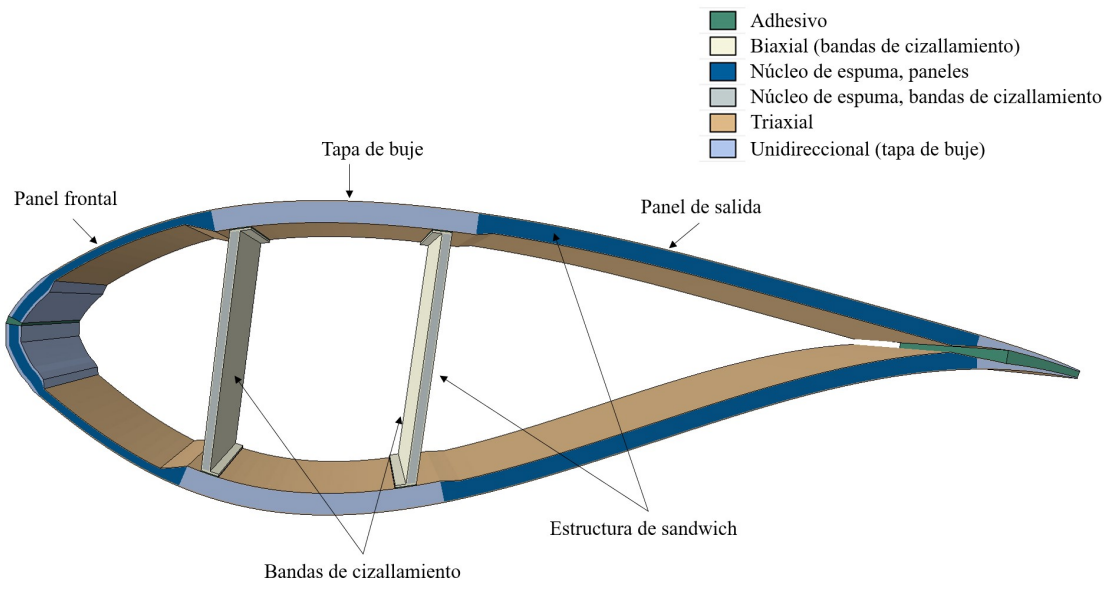

Figure 5: Componentes y materiales de la sección de pala de aerogenerador 3D. Figura basada en la referencia [4].

Por otra parte, se realiza un análisis de fallos de la pala para estudiar qué materiales fallan en condiciones de viento extremo. Los materiales compuestos, el núcleo de espuma y los materiales adhesivos pueden fallar durante la carga, ya que la estructura de la pala

está sometida a momentos de flexión en las direcciones x e y. El principal componente de la estructura de la pala responsable de soportar estas cargas son las tapas de buje, que están unidas entre sí por las bandas de cizallamiento. En este trabajo se evalúa la delaminación del laminado compuesto unidireccional (UD) y el aplastamiento del núcleo de espuma. Para evaluar el fallo en el laminado compuesto unidireccional, se empleará el criterio de fallo por deformación máxima. Por otro lado, también se evaluará el fallo por aplastamiento del núcleo de espuma en las estructuras sándwich.

Resultados

Se han realizado varios casos para comprobar el rendimiento de la interfaz desarrollada. En los casos 1 y 2 se parte de una pala de un aerogenerador nueva, perfecta. En el caso 1, las cargas aerodinámicas correspondientes a las mediciones de velocidad del viento obtenidos en datos reales se aplican a la sección 3D de la pala. A continuación, se realiza un análisis de sensibilidad para encontrar los valores mínimos de desplazamiento rotacional en las direcciones x e y que provocan daños en la estructura de la pala. El caso 2 refleja la situación en la que la estructura de la pala está sometida a un perfil de viento que produce las condiciones de carga mínimas para inducir daños en la estructura de la pala. Por último, tanto para el caso 3 como para el caso 4 se ha cambiado el material del núcleo de espuma utilizado en las estructuras sandwich por otro con propiedades mecánicas inferiores a las utilizadas en el diseño inicial de la estructura de la pala, y los perfiles de viento utilizados para los casos 1 y 2 se aplicarán de nuevo a la estructura de la pala modificada.

El caso 4 es el único en el que se inducen daños en la estructura de la pala, ya que el núcleo de espuma de los paneles frontal y de salida de la pala experimentan una deformación plástica, como se muestra en la Figura 6. Dado que la estructura de la pala presenta daños permanentes, es necesario calcular las propiedades de rigidez con el software 3D de elementos finitos y actualizarlas en la herramienta aeroelástica.

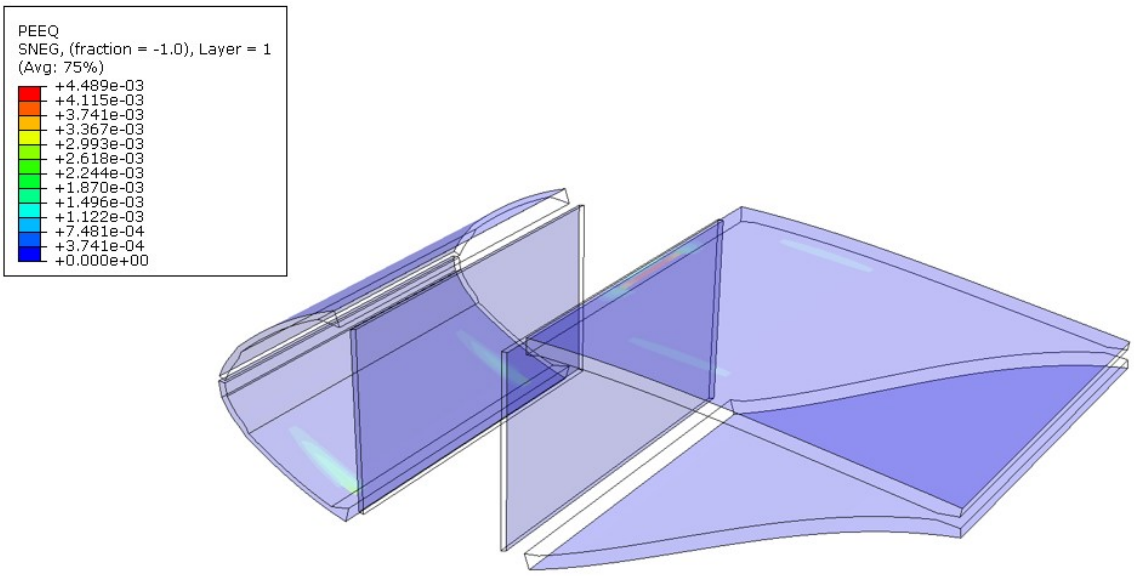

Figure 6: Caso 4. Deformación plástica en el material del núcleo de espuma de la estructura de la pala.

Tanto en el caso 3 como en el 4, se elige una espuma extremadamente ligera para estudiar la degradación de las propiedades de rigidez cuando se inducen daños en la

estructura de la pala, con el fin de analizar la importancia de actualizar las propiedades de rigidez cuando se producen daños, ya que las cargas aerodinámicas se verán afectadas por este cambio en las propiedades estructurales. Sin embargo, la degradación sólo se produce en el caso 4, bajo condiciones de viento más extremas.

Conclusiones

El propósito de este estudio es acoplar una herramienta aeroelástica con un software 3D de elementos finitos a través de una interfaz desarrollada en MATLAB para estudiar la posible degradación de las propiedades de rigidez de las palas de aerogeneradores cuando se inducen daños en la estructura de las mismas. En condiciones meteorológicas normales no deberían inducirse daños en las estructuras de las palas. Sin embargo, su comportamiento bajo condiciones extremas de viento es incierto dado que se encuentran en un escenario que está fuera de sus límites de diseño.

El estudio demostró que la estructura de la pala del aerogenerador elegido tiene unas especificaciones de diseño excelentes junto con una buena elección de materiales, ya que es capaz de soportar velocidades de viento extremas. Se partió de una estructura de pala nueva y perfecta, sin tener en cuenta las cargas de fatiga, los defectos de fabricación o la degradación de la pala, y sin daños inducidos en la pala.

Sin embargo, para probar el rendimiento de la interfaz desarrollada, se debilitó el material del núcleo de espuma en la estructura de la pala, con el fin de inducir daños en la estructura de la pala y estudiar la degradación de las propiedades de rigidez. En este escenario, se detectó la degradación de las propiedades de rigidez de la pala, y la interfaz actualizó correctamente los resultados en la herramienta aeroelástica HAWC2. De este modo, se ha dado un paso más hacia el diseño integrado de aerogeneradores en el que se tienen en cuenta tanto el contexto aeroelástico como el estructural de las palas de los aerogeneradores.

La idea que sustenta el desarrollo de esta interfaz crea un valor añadido para la comunidad investigadora, ya que ayuda a predecir el comportamiento de las palas de los aerogeneradores en determinadas condiciones de viento. La interfaz puede ayudar en el proceso de decisión de reparar una pala de aerogenerador antes o después de la llegada de una tormenta.

3D BLADE MODEL UPDATING BY COUPLING HAWC2 AND ABAQUS

Author: Castilla Mena, María Luz.

Supervisor: Chen, Xiao.

Collaborating Entity: Technical University of Denmark (DTU).

PROJECT SUMMARY

Introduction

Problem Statement

Nowadays, we are currently living in a world where the energy demand is expanding and there is a great concern about getting clean energy from renewable sources. Wind energy has become a fundamental element of the electricity grid, and more wind turbines are being constructed in coastal areas where there is a high energy demand and an ample wind resource. As a result, wind turbines are more exposed to high wind conditions such as typhons and hurricanes that pose a significant danger to its structural integrity. Figure 7, taken from reference [1], shows how a tornado puts the structural response of a wind turbine blade at the limit. The tornado took place in Crowell, Texas on May 4, 2022. It is evident how much a wind turbine blade may bend in these strong winds because of the significant deflections it experiences, and damage may be induced in the blade under these conditions. However, not only are offshore wind turbines affected by extreme weather conditions but also land-based wind turbines.

Figure 7: Wind turbine blade deflection under the influence of a storm. Figure taken from reference [1].

As wind turbines are exposed to external conditions it is inevitable that their performance will deteriorate over time. It is important to know that, in the aeroelastic context of a wind turbine, both the aerodynamic loads and the structural properties influence each other. The aerodynamic loads can make the blade deform and this deformations change the direction of the wind flow, changing the aerodynamic loads. This is what is called a coupled problem.

Under extreme wind conditions as the one shown in Figure 7, wind turbines are exposed to a situation out of their design limits, and it is uncertain how it will react. Damage can be induced in the blade structure and the stiffness properties of the blade can be

degraded due to the extreme aerodynamic loads. If not replaced on time, it could potentially damage the whole wind turbine structure.

State of the art

Aeroelastic tools are used to calculate the time response of a wind turbine under given wind conditions by computing the aerodynamic loads in an easy and simple way. The approach followed by aeroelastic tools is to divide the wind turbine blade structure into sections, with each section being modelled as a beam element (see Figure 8). The aeroelastic tool sees each blade section as a single line, with no height or width, and with constant stiffness properties. With this approach, nonlinearities associated with geometry, material or composite layup are not considered.

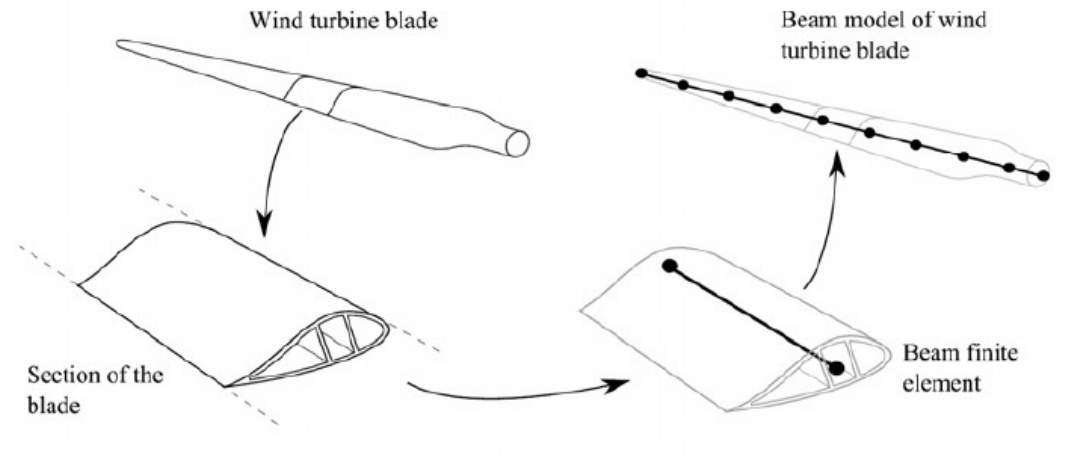

Figure 8: Beam element approach. Figure taken from reference [2].

However, under extreme weather conditions in which damage can be induced in the blade structure, this beam element approach does not take into account the structural degradation. The assumption is not sufficient to accurately compute the aerodynamic loads because it does not take into account the geometry of the structure, or if there is delamination in the composite material or foam core crush.

Project Goals

The idea behind this study is to develop an interface that couples the aeroelastic tool HAWC2 with the 3D FE software ABAQUS to consider the stiffness properties degradation when damage is induced in a wind turbine blade section under extreme wind conditions. With this interface, interactions between aeroelastic and structural systems are considered.

If under extreme wind conditions damage is induced in the blade structure, the 3D FE software will calculate the stiffness properties on a 3D blade section and the interface will update them into the aeroelastic tool HAWC2 to compute the corresponding aerodynamic loads. By following this approach, accurate simulations corresponding to extreme wind scenarios can be achieved, therefore helping predict the wind turbine's behaviour under extreme wind conditions.

Methodology

The overall workflow of the interface is shown in Figure 9. The interface will be developed in MATLAB.

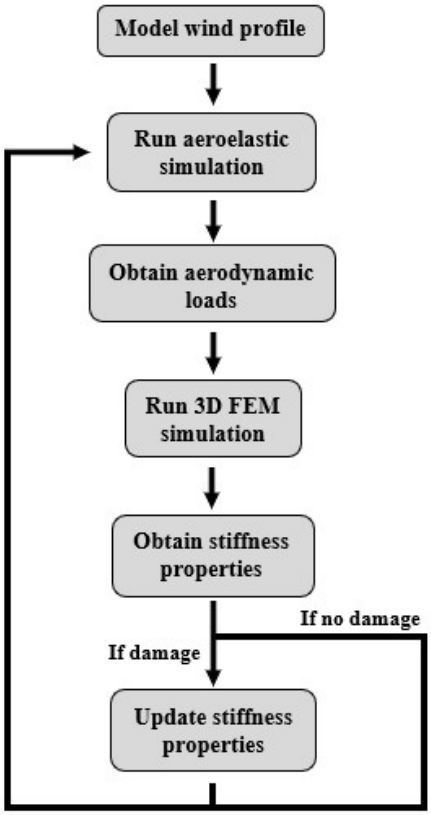

Figure 9: Overall workflow of the MATLAB interface.

The overall workflow of the MATLAB interface consists of the following six main steps.

- **Step 1: Model wind profile**. First, the extreme wind profile needs to be described so that it can be modelled by the aeroelastic simulation tool and use it as an input.
- **Step 2: Run aeroelastic simulation**. Once the extreme wind profile is modelled, the aeroelastic simulation is run and the aerodynamic loads in the wind turbine blades are computed.
- **Step 3: Obtain aerodynamic loads**. The interface reads the results obtained from the aeroelastic simulations.
- **Step 4: Run 3D FE simulation**. Subsequently, the aerodynamic loads are applied to the 3D blade structure, the 3D FE simulation is run and the structural properties are obtained.
- **Step 5: Obtain stiffness properties**. The interface reads the results obtained from the 3D FE simulations and computes the new stiffness properties of the wind turbine blade sections.
- **If failure is found on the blade stucture**:
  - **Step 6: Update stiffness properties**. The interface updates the stiffness properties in the aeroelastic simulation tool. As a result, new aerodynamic loads can be computed again by running the aeroelastic simulation.

- **If no failure is found on the blade structure**. No update of stiffness properties is needed and the aerodynamic loads can be computed again by running the aeroelastic simulation tool.

To run the interface and perform the simulations, both the aeroelastic and the 3D FE set-ups need to be defined. For the aeroelastic set-up, the wind turbine specifications need to be defined in order to do the simulations, and the wind profile needs to be modelled. For the 3D FE software ABAQUS set-up, the 3D blade section needs to be defined, where the stiffness properties will be calculated, and a blade failure analysis will be performed.

Regarding the wind turbine specifications for the aeroelastic set-up, the DTU 10MW Reference Wind Turbine has been selected as the wind turbine for this study. For the structural design, the blade has been divided in 51 sections across its length. Each section has been modelled as beam elements with constant stiffness properties, corresponding to its respective cross-section.

In addition, an extreme wind profile needs to be modelled, as the objective is to induce damage in the blade structure. According to the Saffir-Simpson scale, wind profiles with a mean wind speed of around 33-43 m/s can produce damage to buildings. In addition the wind profile should have a remarkable wind gust, as storms are characterized to have sudden increase of wind speeds. Real data measurements were chosen that fulfil these characteristics, corresponding to a mast in Skipheya, the Norwegian island of Froya. However, in order to model the wind profile in the aeroelastic tool HAWC2, there are some requirements. The wind profile needs to be modelled at hub height, and the 3 wind field components (u, v, and w components) are needed to model the wind profile. The u component is obtained from the real data measurements, whereas the v and w components are calculated using a turbulence field generation package. Using this tool, a constrained turbulence box can be simulated to recreate the flow structures. The turbulence box is the tool used to simulate the wind profile, it holds inside all the turbulence field and assumes it moves with the mean wind speed towards the wind turbine. The turbulence box is generated by constraining a single component, which in this case is the u component, as it is the one obtained from the data file turbulence measurements. Figure 10 shows how a turbulence box looks like and the parameters needed to define it.

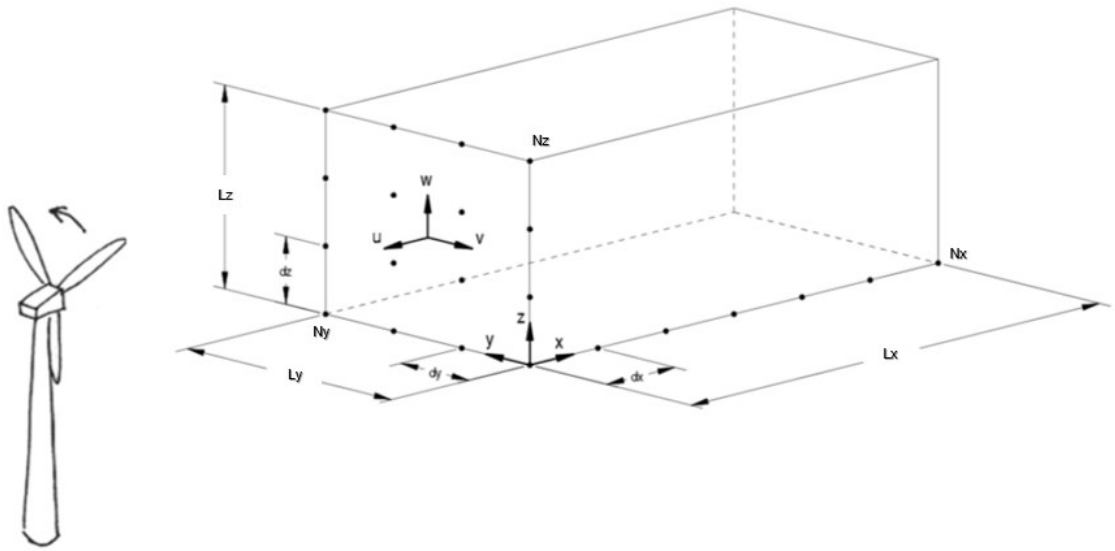

Figure 10: Dimensions of the turbulence box. Figure taken from reference [3].

According to the 3D FE set-up, the 3D blade section needs to be defined. The 3D blade section that has been used for this study has been modelled according to the DTU 10MW Reference Wind Turbine structural design. The blade is made from glass fiber reinforced composites and sandwich structures with foam core material, as shown in Figure 11. If damage is induced in the blade section, the stiffness properties will be recalculated for the blade structure with the 3D FE software ABAQUS, and the interface will update them into the aeroelastic tool HAWC2 for the next calculation of aerodynamic loads.

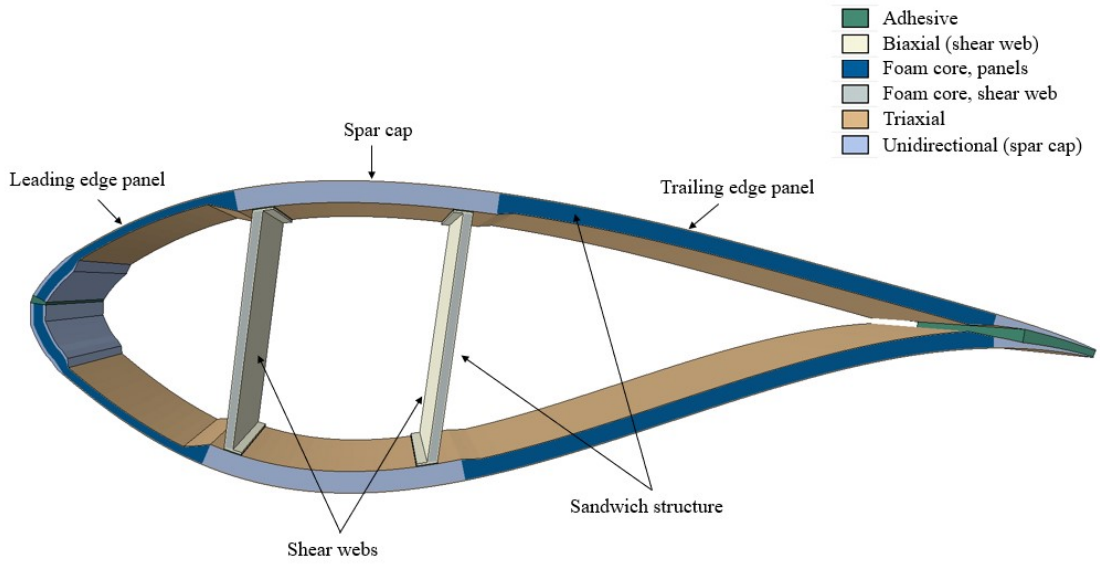

Figure 11: Components and materials of the 3D wind turbine blade section. Figure based on reference [4].

Furthermore, a blade failure analysis is performed to study which materials fail under extreme wind conditions. The composites, foam core and adhesive materials can fail during the loading, as the blade structure is subject to bending moments in both the x and y directions. The main blade structure component that is responsible for supporting these loads are the spar caps, which are coupled together by the shear webs. In this work, the delamination of the unidirectional (UD) composite laminate and foam core crushing are evaluated. To evaluate the failure in the UD composite laminate, the maximum strain failure criterion will be employed. On the other hand, the foam core crush failure will also be evaluated in the sandwich structures.

Results

Several case studies have been conducted to test the performance of the developed interface. A perfect new blade is assumed in Case study 1 and Case study 2. For Case study 1 the aerodynamic loads corresponding to the real data measurements are applied to the 3D FE blade section. A sensitivity analysis is then carried out to find the minimum rotational displacements values in both x and y directions that induce damage to the blade structure. Case study 2 reflects the situation where the blade structure is subject to a wind profile that produces the minimum loading conditions to induce damage to the blade structure. Finally, for both Case study 3 and Case study 4 the foam core material used in the sandwich structures has been changed to another with lower mechanical properties than the ones used in the initial design of the blade structure, and the wind profiles used for Case study 1 and 2 will be applied again to the modified blade structure.

Case 4 is the only case in which damage is induced in the blade structure, as the foam core in both the leading and the trailing panels experience plastic deformation, as shown in Figure 12. Since the blade structure has permanent damage, the stiffness properties need to be computed with the 3D FE software and updated into the aeroelastic tool.

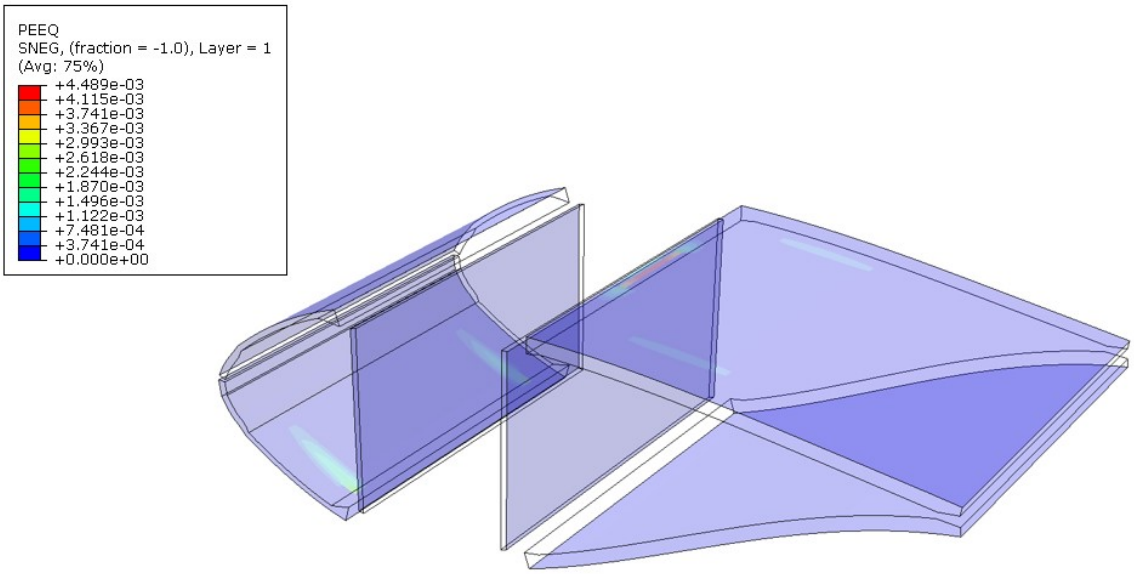

Figure 12: Case study 4. Plastic deformation in the foam core material of the blade structure.

For both Case studies 3 and 4, an extremely light foam is chosen to study the degradation of stiffness properties when damage is induced in the blade structure, in order to analyse the significance of updating the stiffness properties when damage occurs, as the aerodynamic loads will be affected by this change in the structural properties. However, degradation only occurs in Case study 4, under more extreme wind conditions.

Conclusions

The purpose of this study is to couple an aeroelastic tool with a 3D FE software through an interface developed in MATLAB to study the possible degradation of wind turbine blade stiffness properties when damage is induced in the wind turbine blade structure. Under normal weather conditions there should be no induced damage in blade structures. However, their behaviour under extreme wind conditions is uncertain given that they are in an scenario that is outside of their design limits.

The study showed that the blade structure for the chosen wind turbine has great design specifications along with a good choice of materials, as it is capable to withstand extreme wind speeds. A perfect new blade structure was assumed, without considering fatigue loads, manufacturing flaws or blade degradation, and no damage was induced in the blade.

However, to test the performance of the developed interface, the foam core material in the blade structure was weakened, in order to induce damage in the blade structure and study the degradation of the stiffness properties. Under this scenario, degradation of the blade stiffness properties was found, and the interface correctly updated the results into the aeroelastic tool HAWC2. This way, a step has been moved towards the integrated design of wind turbines where both the aeroelastic and structural context of wind turbine blades are considered.

The idea behind the development of this interface creates added value to the research community, as this interface helps in the wind turbine blade behaviour prediction under certain wind conditions. The interface can help in the decision process of repairing a wind turbine blade before or after the upcoming of a storm.

DTU Wind

3D blade model updating by coupling HAWC2 and ABAQUS

María Luz Castilla Mena

DTU Wind-M-0581

March 2023

Author: María Luz Castilla Mena

Title:
3D blade model updating by coupling HAWC2 and ABAQUS

DTU Wind-M-0581
March 2023

Project period:
September 2022 - March 2023

ECTS: 35

Education: Master of Science

Supervisor(s):

Xiao Chen
Xingyuan Miao
Ju Feng
DTU Wind and Energy Systems

Remarks:
This report is submitted as partial fulfillment of the requirements for graduation in the above education at the Technical University of Denmark.

Technical University of Denmark
Department of Wind and Energy Systems
Frederiksborgvej 399
DK-4000 Roskilde
www.wind.dtu.dk

DTU Wind and Energy Systems is a department of the Technical University of Denmark with a unique integration of research, education, innovation and public/private sector consulting in the field of wind and energy. Our activities develop new opportunities and technology for the global and Danish exploitation of wind and energy. Research focuses on key technical-scientific fields, which are central for the development, innovation and use of wind energy and provides the basis for advanced education.

TECHNICAL UNIVERSITY OF DENMARK

Abstract

DTU Wind and Energy Systems

Master of Science in Wind Energy

3D blade model updating by coupling HAWC2 and ABAQUS

by Maria Luz Castilla Mena

The wind energy sector has developed considerably in terms of technology improvements, cost reductions, and implementation. More wind turbines are being constructed in coastal areas where there is a high energy demand and an ample wind resource. As a result, extreme wind conditions such as typhoons and hurricanes pose a significant danger to the structural integrity of wind turbines. Under extreme weather conditions, damage may be induced in wind turbine blades and their stiffness properties may experience significant degradation. In the aeroelastic context of a wind turbine, it is important to consider the mutual effects of the aerodynamic loads and the structural properties. An approach to improve the analysis of a wind turbine blade's behaviour under extreme wind conditions is to couple software for aeroelastic and structural simulations. This work presents the coupling of the aeroelastic simulation tool HAWC2 and the 3D FE software ABAQUS through an interface developed in MATLAB. This interface will link the aerodynamic loads computed by the aeroelastic tool HAWC2 and use them as an input to calculate the structural properties on 3D FE blade sections. If damage is encountered on the 3D blade structure, the stiffness properties will be updated into the aeroelastic tool to compute the new aerodynamic loads. This way, the interface considers the degradation of the stiffness properties of wind turbine blade structures in the calculations of aerodynamic loads, taking into account structural non-linearities associated with geometry and composite layup that are neglected in the beam theory model used by the aeroelastic tool HAWC2. In other words, interactions between aerodynamic loads and structural properties of blade structures in the time response of a wind turbine are achieved with this interface. An extreme wind profile based on real wind turbulence measurements has been modelled for this study, and the DTU 10 MW Reference Wind Turbine has been employed.

Keywords: Extreme wind, structural integrity, aeroelastic modelling, turbulence, finite element analysis

Acknowledgements

First of all, I would like to express my gratitude to all my supervisors. Xiao Chen and Xing-Yuan Miao, my main supervisors, thank you for believing in me and showing interest and support throughout all the project. As for my co-supervisors, Ju Feng and Suguang Dou, thank you for transferring your knowledge about the HAWC2 aeroelastic simulation tool and the turbulence modelling of wind profiles. All your help is reflected in the development of this project.

In addition, I would like to thank my parents for always showing support in every decision I have faced in my life. Even though we are not in the same country, I always feel you close. I would also like to thank my friends in both Denmark and Spain for all the encouragement received during these last two years. Especially to my roommates, who have been by my side in all the process, making me feel home.

Last but not least, I would like to show my gratitude to DTU and my home university in Spain, Universidad Pontificia Comillas ICAI, for allowing me participate in the TIME programme, with which I had the opportunity to study the MSc in Wind Energy in Denmark. Looking forward to see what the future holds.

Contents

List of Figures

List of Tables

List of Symbols

Turbulence		
Lx	Length of the turbulence box in longitudinal (x) direction	m
Ly	Length of the turbulence box in transverse horizontal (y) direction	m
Lz	Length of the turbulence box in transverse vertical (z) direction	m
Nx	Dimension of the turbulence box in longitudinal (x) direction	-
Ny	Dimension of the turbulence box in transverse horizontal (y) direction	-
Nz	Dimension of the turbulence box in transverse vertical (z) direction	-
dx	Spacing between data points along the x-coordinate	m
dy	Spacing between data points along the y-coordinate	m
dz	Spacing between data points along the z-coordinate	m
L	Mann model turbulence length scale parameter	-
Γ	Mann model turbulence anisotropy parameter	-
$\alpha\epsilon$	Mann model turbulence parameter	-
Structural		
E	Elasticity modulus	N/m^2
G	Shear modulus	N/m^2
A	Cross-sectional area	m^2
Ix	Moment of inertia in the x direction	m^4
Iy	Moment of inertia in the y direction	m^4
J	Torsional moment of inertia	m^4
k_x	Shear factor for force in the principal bending xe direction	-
k_y	Shear factor for force in the principal bending ye direction	-

1 Introduction

Wind energy is currently a fundamental element of the electricity grid, subject to regulations for power quality and reliability. The wind energy sector has developed considerably in terms of technology improvements, cost reductions, and implementation. Due to these factors, wind energy is expected to produce 50% of power in Europe by 2050, 44% in North America, and more than 30% in Greater China, Latin America, and South East Asia [5].

In a world where energy demand is expanding and there is a growing feeling of urgency about environmental issues, an increasing number of countries are turning to offshore wind energy to meet these difficulties. While offshore wind energy brings significant potential, it also poses considerable concerns [6], [7]. More wind turbines have been constructed in coastal areas where there is a high energy demand and an ample wind resource. As a result, high wind conditions such as typhoons and hurricanes pose a significant danger to wind turbine structural integrity [8]. Figure 1.1, taken from reference [9], shows an offshore wind farm under extreme weather conditions. On the basis of in-depth investigation and phenomenological evaluation, wind turbine structural failure incidents brought on by strong winds have been regularly documented in recent years [7].

Figure 1.1: Offshore wind turbines under the influence of a storm. Figure taken from reference [9].

However, not only are offshore wind turbines affected by extreme weather conditions but also land-based wind turbines, although less frequently. Figure 1.2, taken from reference

[1], shows how a tornado puts the structural response of a wind turbine blade at the limit. The tornado took place in Crowell, Texas on May 4, 2022.

Figure 1.2: Wind turbine blade deflection under the influence of a storm. Figure taken from reference [1].

As wind turbines are exposed to external conditions it is inevitable that that their performance will deteriorate over time. In the aeroelastic context of a wind turbine, it is important to emphasize that both the aerodynamic forces and the structural flexibility influence each other. When the aerodynamic forces change, the wind turbines deformations change. These deformations change the blades orientation with respect to the wind flow, making the aerodynamic forces change again. This is what it is called a coupled problem, in which both the aerodynamic forces and the structural deformations influence each other. Weak sections can appear in the blades and, under extreme wind conditions, such as storms, blades could fail.

The aim of this study is to determine if, under extreme weather conditions, the structural properties of wind turbine blades are significantly degraded when their interaction with aerodynamic loads is considered. For this purpose, an interface is developed to couple an aeroelastic tool together with a 3D finite element (FE) software, in order to compute the stiffness properties using high-fidelity 3D finite element modelling, to account for structural non-linearities associated with geometry and composite layup. It is important to emphasise that this possible degradation of the structural properties of wind turbine blades may occur under extreme weather conditions, as these are situations outside the design limits and it is uncertain how the wind turbine might react. Under normal weather scenarios there would be no significant change in the structural properties of wind turbine blades.

1.1 Theoretical background

Wind turbines are vulnerable to storms because the maximum wind speeds that can be reached in those conditions may surpass wind turbines' designed limitations [10]. Loss of blades and buckling of the supporting tower are two possible failure scenarios under this circumstances. Blades are often rather simple to replace, although their loss might result in additional structural damage [11].

To understand the reason why exceeding the design limits of wind turbines is undesirable, the power curve of a wind turbine needs to be explained. The power curve displays a wind turbine's power production in relation to the mean wind speed, as shown in Figure 1.3. The cut in speed is the wind speed at which the blades start rotating and generating power. As wind speed increases, more electricity is generated until the rated wind speed

is reached. At this point, the wind turbine generates its maximum, or rated power. The power generated by the wind turbine remains constant at this point as the wind speed continues to increase, until the cut out speed is reached. The cut out speed is the maximum wind speed at which the generator is designed to produce usable energy. When the cut out wind speed is reached, the wind turbine shuts down to avoid excessive strain on the rotor [9].

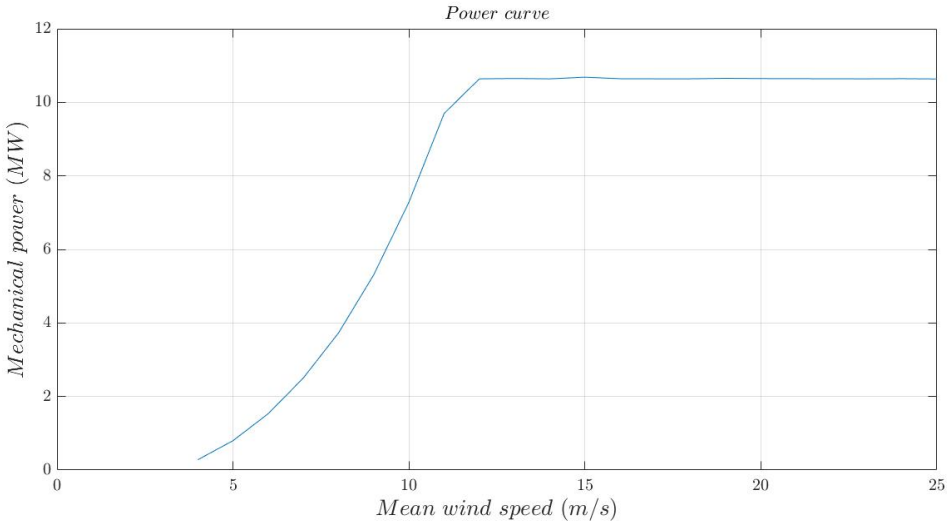

Figure 1.3: DTU 10MW Reference Wind Turbine Power Curve.

The power curve displayed above corresponds to the DTU 10 MW Reference Wind Turbine. The data was taken from reference [12]. In this case, the cut-in wind speed is 4 m/s, the rated wind speed is 11.4 m/s, the cut out wind speed is 25 m/s, and the rated power is 10 MW [13].

Every wind turbine is equipped with an anemometer to measure wind speed and a wind vane to monitor wind direction. The wind turbine shuts off automatically when the anemometer detects wind speeds greater than the cut-out speed. Furthermore, when the rated wind speed is detected, the blades begin to feather. This means that the blades edge starts facing to the wind with the aim of reducing their surface area. Even though it is uncommon, the blades can sometimes be locked down to withstand strong winds. This is called parked condition. The yaw driver, which is housed in the wind turbine's nacelle, continues to point the rotor into the wind despite this switch off, even when weather patterns change as they pass by [9].

Following the wind turbine design standard IEC61400-3 Design Load Cases (DLCs) [14], the DLCs are specified for each design situation by their related metocean conditions and control system operational behavior, fault scenarios, and other occurrences. Specifications are given and recommended to be followed when encountering one of these scenarios. Design situations 6.x and 7.x reflect the parked condition without and with fault scenarios, respectively [15].

These are common ways to act when a wind turbine is under the influence of a storm. However, they do not allow to predict if a wind turbine blade will be potentially damaged under the extreme weather conditions. As previously remarked, in these circumstances the relation between the aerodynamic loads and the structural properties may lead to a possible degradation of the structural properties of the blade. A blade is relatively easy

to replace, but if not replaced on time it could potentially damage the whole wind turbine structure.

1.2 State of the art

Given the fact that under extreme wind conditions the behaviour of a wind turbine blades is uncertain, to predict the damage in wind turbine blade structures, Jeong *et al.* [16] consider an approach to detect damage at an early stage through the real-time monitoring using digital image correlation (DIC) to predict the location of the damage. In Chen *et al.* [17], infrared thermography, digital image correlation, and acoustic emission (AE) are used to identify and monitor damage, allowing to identify imminent structural failure and steady damage growth.

Coupling an aeroelastic tool with a 3D FE software can also help in predicting the behaviour of wind turbine blade structures. This link between different programmes is needed because the aeroelastic tool models the wind turbine structure as beam elements to calculate the aerodynamic loads in a more efficient manner. The aeroelastic tool makes beam theory assumptions and considers a wind turbine blade section as a beam element, where neither the geometry nor the composite layup of the blade structure is considered. Using a 3D FE software helps in a more exact computation of the stiffness properties of the blade. In Larsen *et al.* [18] the effects of including large blade deflections in aeroelastic calculations are considered, using non-linear approaches to quantify these effects. However, non-linearities dealing with large blade deflection such as material properties, buckling or delamination are not part of the analysis. The non-linearity addressed in the study is the result of computing the inertia at the deflected region and imposing loads on the deflected structure.

Integrating several software that are dedicated to particular aspects of wind turbine design and analysis is a step towards integrated design of wind turbines [19]. In Kaufer *et al.* [20], integrated analysis is done for offshore wind turbines. Flex5, a commonly used wind turbine simulation tool, and Poseidon, a finite element software used for structural analysis, are coupled together with the purpose of combining aerodynamic and hydrodynamic loading taking into consideration the dynamic response of the support structure. In this case both software are coupled together without the need of an external software. In Garzon *et al.* [19], the aeroelastic tool HAWC2 and MATLAB/Simulink have been linked together to simulate a semi-variable speed wind turbine. This allows for study of the interactions between the aeroelastic, structural, electrical, and control systems of wind turbines and the grid. HAWC2 simulates the aeroelastic behavior of wind turbines in the time domain, while MATLAB/Simulink is designed to perform control and power system simulations. In Papazafeiropoulos. *et al.* [21], the link between 3D FE software ABAQUS and MATLAB is created to take into consideration finite element modeling and mathematical analysis. This connection provides up new prospects for mathematical optimization, statistical analysis, and results post-processing, among many other potential applications.

In this study, an interface is developed in MATLAB to couple the aeroelastic tool HAWC2 together with the 3D finite element (FE) software ABAQUS. The interface will use the aerodynamic loads computed by the aeroelastic tool and will update the low-fidelity beam theory computed stiffness properties with the ones obtained with a high-fidelity 3D finite element approach, taking into account the geometry of the blade section and the composite layup. Blade failure analysis will also be developed to consider delamination in composite materials and foam core crush. The idea behind the development of this interface is

to predict whether or not a blade is going to fail in the upcoming of extreme weather conditions and assess the option whether the blade should be replaced, for instance, before or after a storm. Simulations will be carried out linking both software and, if damage is induced in the blade structure, the interface will update the structural properties of the blade and therefore, the aerodynamic loads. This way, degradation of the stiffness properties will be considered during the wind turbine's response in the time domain. Figure 1.4 shows a general overview of the interface's workflow.

Figure 1.4: Overview of the interface's workflow presented in this thesis.

1.3 Overview of the thesis

After a brief introduction to the theoretical background and the state of the art of the project in Chapter 1, Chapter 2 will focus on the methodology, where the overall workflow and structure of the developed interface that links both software will be explained, together with an explanation of the aeroelastic and structural models. Chapter 3 includes the aeroelastic and the structural modelling setup, the numerical setup used in all software to the development of the simulations that prove that the interface works, along with the computer environment settings. It includes the wind turbine employed for the study, how an extreme wind profile is modelled, and an overview of the 3D blade section modelled in the 3D FE software. The description of the case studies performed to test the operation of the developed interface is given in Chapter 4, along with a discussion of the obtained results. In Chapter 5, the conclusions are summarized and a future improvement is suggested.

2 Methodology

In order to analyse blade structural response in operational wind turbine environments, an interface is developed to link the aeroelastic tool HAWC2 and the 3D FE software ABAQUS. The interface is developed in MATLAB [22]. With this interface, interactions between aeroelastic and structural systems are considered, since both the aerodynamic loads and the structural response influence each other. The aerodynamic loads have impact on the structural properties of the wind turbine, and changes in the structural properties also influence the aerodynamic loads.

Under extreme weather conditions damages can be induced in the blade structure, reducing the stiffness of the structure. The change in the structural properties leads to a change in the aerodynamic loads that the aeroelastic tool would not notice when using the beam element assumptions. Updating the stiffness properties in the aeroelastic tool with a 3D finite element approach can make a difference in the calculation of a wind turbine blade time response. The main purpose of developing this interface is to investigate the response of blade structure under extreme wind events taking into account the possible degradation of stiffness properties, to see whether the change in the stiffness properties affects the time response of a wind turbine blade. The overall workflow of the MATLAB interface is shown in Figure 2.1.

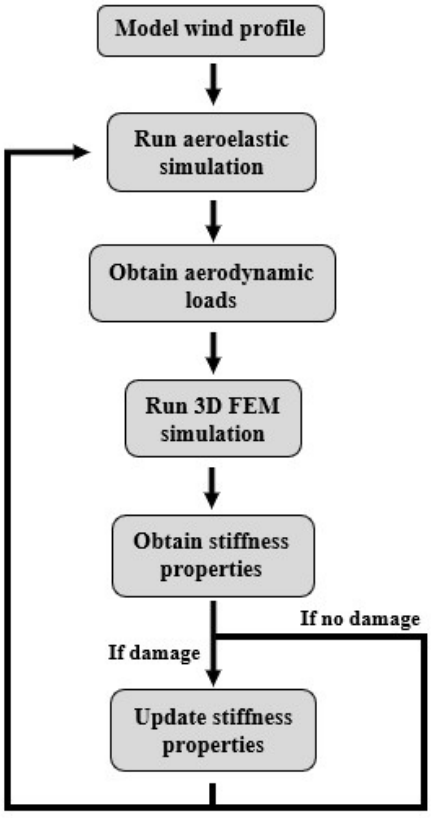

Figure 2.1: Overall workflow of the MATLAB interface.

2.1 Workflow of the interface

As shown in Figure 2.1, the overall workflow of the MATLAB interface consists of the following six main steps.

- **Step 1: Model wind profile**. First, the extreme wind profile needs to be described so that it can be modelled by the aeroelastic simulation tool and use it as an input.
- **Step 2: Run aeroelastic simulation**. Once the extreme wind profile is modelled, the aeroelastic simulation is run and the aerodynamic loads in the wind turbine blades are computed.
- **Step 3: Obtain aerodynamic loads**. The interface reads the results obtained from the aeroelastic simulations.
- **Step 4: Run 3D FE simulation**. Subsequently, the aerodynamic loads are applied to the 3D blade structure, the 3D FE simulation is run and the structural properties are obtained.
- **Step 5: Obtain stiffness properties**. The interface reads the results obtained from the 3D FE simulations and computes the new stiffness properties of the wind turbine blade sections.
- **If failure is found on the blade stucture**:
  - **Step 6: Update stiffness properties**. The interface updates the stiffness properties in the aeroelastic simulation tool. As a result, new aerodynamic loads can be computed again by running the aeroelastic simulation.
- **If no failure is found on the blade structure**. No update of stiffness properties is needed and the aerodynamic loads can be computed again by running the aeroelastic simulation tool.

This workflow allows to simulate the time response of wind turbine blades under operational wind turbine environments and, if damage is induced on the blade structure, it allows to update the stiffness properties using 3D FE models of blade sections. In short, it allows to analyze structural behaviours of blade structures in detail during a simulation. In each iteration, structural failures will be checked in the blade. Steps two to six are repeated until the simulation time is reached.

2.2 Structure of the interface

To couple the aeroelastic simulation with 3D FE simulation, the structure shown in Figure 2.2 is used in the interface. It consists of a main code where the entire simulation is conducted. Within the main code, functions are called to perform specific tasks. This is done with the intention of making the main code simpler and clearer. The pseudocodes for all the codes can be found in the Appendix B.

Inside the main code, and after the initialization, the extreme wind profile is next to be specified. Real wind data measurements will be read using the function `readwindprofile` and turbulence files will be generated. In this work, HiperSim is used to generate the turbulence files for the aeroelastic tool to model the wind profile. A detailed explanation of the generation of turbulence files is found in Section 3.1.2.

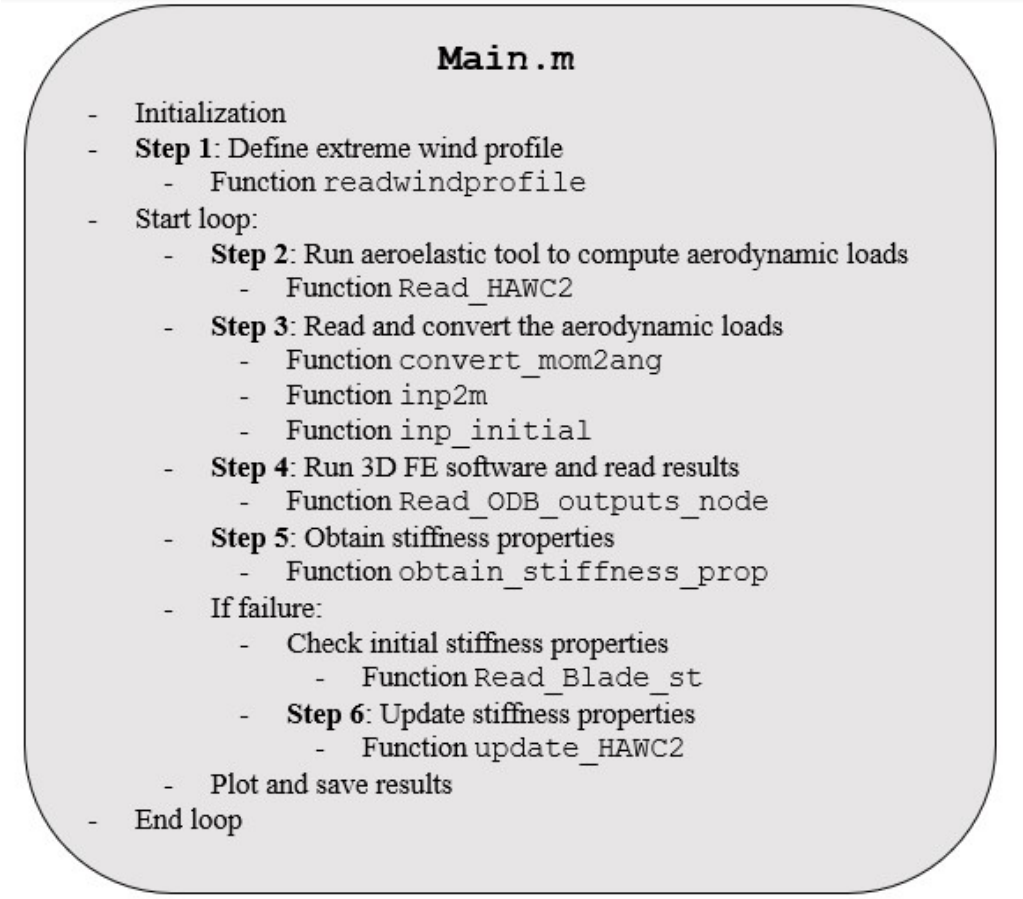

Figure 2.2: Structure of the MATLAB interface.

The aeroelastic tool will then be run by the interface to compute the aerodynamic loads corresponding to the modelled wind profile, and the function `Read_HAWC2` will read and store the following results:

- Time vector of the simulation (s).
- Wind speed in the x, y, and z direction at the hub height (m/s).
- Cross-sectional forces and moments in the specified location of the blade (N and N m, respectively).

Wind speed results are collected and compared to the real wind measurements to demonstrate that the aeroelastic tool accurately modelled the extreme wind profile. Regarding the aerodynamic loads, cross-sectional forces will be neglected in the blade section analysis and will focus instead on the cross-sectional moments Mx and My, also referred to as bending moment in the flapwise direction and bending moment in the edgewise direction, respectively. Figure 2.3 shows how the flapwise (Mx) and edgewise (My) moments look in a wind turbine blade, taken from the reference [23]. The cross-sectional moment Mz, also referred to as torsional moment, is smaller in comparison with the flapwise and edgewise moments and is also neglected from this analysis. Table 3.5 in Section 3.1.2 shows the order of magnitude of the cross-sectional aerodynamic loads.

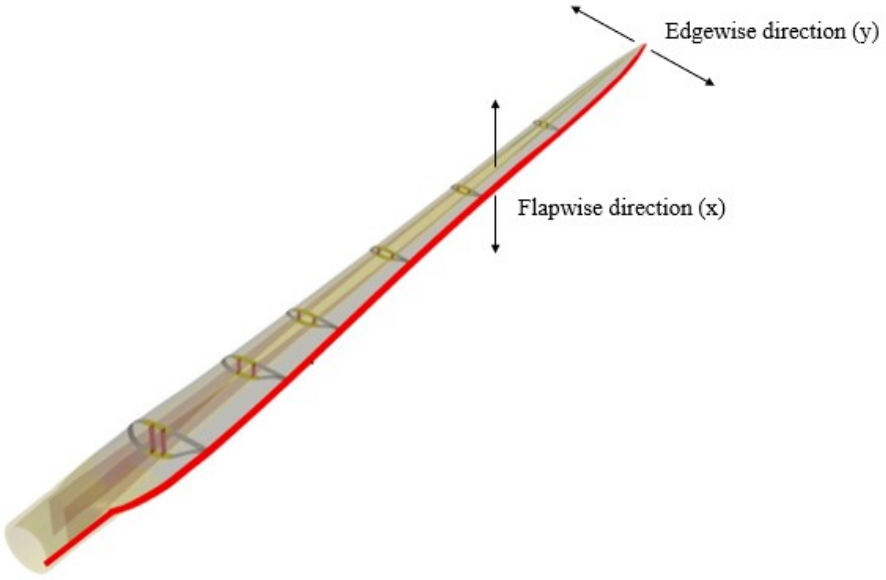

Figure 2.3: Flapwise and edgewise moments in a wind turbine blade. Figure adapted from reference [23].

Given that the modelled blade section is very complex and has many details, to ease the convergence of the structural simulation the cross-sectional moments will be expressed in terms of angular rotations. This implies that rotational displacement will be applied instead of moments to the 3D blade section, and the conversion will be done with the function `convert_mom2ang`. A detailed explanation of how the conversion of moments to angular rotations is done can be found in Section 3.1.3. Function `inp2m` creates the function `inp_initial` which is responsible for writing the input data needed by the 3D FE software. The last mentioned function creates the input file to be read by the 3D FE software.

The next step is to run the 3D FE simulation and read the results obtained using the function `Read_ODB_outputs_node`. Information on stress and strain of the blade section, among others, can be obtained at this point and will be used later for blade failure analysis. The stiffness properties will be obtained using the function `obtain_stiffness_prop`. In Section 3.2.5 the process to obtain the stiffness properties from the 3D blade section model will be described. If damage is found on the 3D blade sections, function `Read_blade_st` will read the current stiffness properties used by the aeroelastic tool and function `update_HAWC2` will update them so that in the next iteration the updated aerodynamic loads can be computed, the ones corresponding to the structural situation of the blade sections at the point. If no damage is found on the blade sections, the loop will jump to the next iteration without updating the stiffness properties. Damage is user-defined in the code as the minimum percentage of degradation of stiffness properties. If the percentage of degradation obtained after running the simulation is above that value, the code detects that damage has been induced in the blade section and will update the stiffness properties in the aeroelastic tool.

With the results obtained from the 3D FE simulation, a blade failure analysis is performed to study the influence of the extreme wind profile in wind turbine blade sections. Foam core crush and delamination of the unidirectional (UD) composite laminate are the two failure scenarios to be checked in this study. Further details are explained in Section

3.2.6. This procedure is not currently implemented in the MATLAB interface but checked manually.

2.3 Aeroelastic model

For this study, HAWC2 (which stands for Horizontal Axis Wind turbine Code 2nd generation) is the aeroelastic tool used to compute the aerodynamic loads. It is a tool for modelling a wind turbine's response in the time domain. This aeroelastic wind turbine simulation tool is currently being developed at DTU Wind [24]. Special focus will be given to the wind model, the aerodynamic model, and the structural model.

The HAWC2 software is used to study the dynamic behaviour of a wind turbine. In the aeroelastic context of a wind turbine, the mutual effects of the aerodynamic forces and the structural properties are considered. The HAWC2 structural formulation is coupled to an aerodynamic model that can compute the aerodynamic forces acting on the blades using the aerodynamic Blade Element Momentum (BEM) model. In addition, HAWC2 software allows to model the extreme wind profile. With the built-in Mann turbulence generator, HAWC2 can generate turbulent wind fields based on site-specific wind data [25].

2.3.1 Wind model

The wind model that HAWC2 employs to reproduce the wind field in which the wind turbine operates is explained in the following subsection. An overview of turbulence and how turbulence fields are generated in HAWC2 is given. The Mann model [26] receives special consideration as it is completely integrated with the HAWC2 software.

It is convenient to distinguish between properties related to the mean wind speed and the turbulence properties. On one hand, the mean wind properties take into account the mean wind speed at hub height, the wind shear (wind velocity profile as function of height), and the wind direction (the positive direction is the wind seen from the wind turbine). On the other hand, turbulence is defined by a turbulence vector field, with a mean value of zero in all directions: u,v and w. The u component represents the direction of the mean wind speed. The perpendicular component is called v, and the vertical direction specified upwards is the w component [27].

HAWC2 turbulence field generation is based on the Mann model formulation [26], as it generates a spatial vector field in cartesian coordinates. The local speed and direction of the flow are represented by a three-dimensional vector at each point of the vector field. The Taylor's assumption is used, also known as frozen turbulence assumption, states that large turbulence structures are transported with the mean wind speed and do not vary over time. Then the Mann model is used, and the solution is the creation of a field that is perfectly correlated between variations in the u, v, and w directions. Isotropic turbulence is assumed, which explains that the length scale and variance level is the same for the three directions [3].

Applying the turbulence model is relatively straightforward, since there are mainly four input parameters. The first parameter is the alpha-epsilon value, $\alpha\epsilon$, which is the one that determines the variance level. The second parameter is the length scale L, matching the most energetic turbulent motions. The third parameter is the shear parameter gamma, Γ, which gives the magnitude of shear. An isotropic turbulence without shear has a Γ value of zero. Last, but not least, the fourth parameter is the high frequency compensation, which relates to the discretization of the vector field [3].

2.3.2 Aerodynamic model

As previously mentioned, HAWC2's aim is to model the aeroelastic response of a wind turbine to external force conditions. The aerodynamic model is based on a Blade Element Momentum (BEM) formulation, a relatively simple model that requires limited computation time. With this model the aerodynamic forces over the wind turbine rotor can be computed in a relatively simple and fast way by combining two levels. The rotor aerodynamics are modeled on the first level, and the steady and unsteady aerodynamic forces acting on the 2D airfoil sections that define each blade element are described in the second level [28]. Figure 2.4 shows a schematic of HAWC2's aerodynamic model.

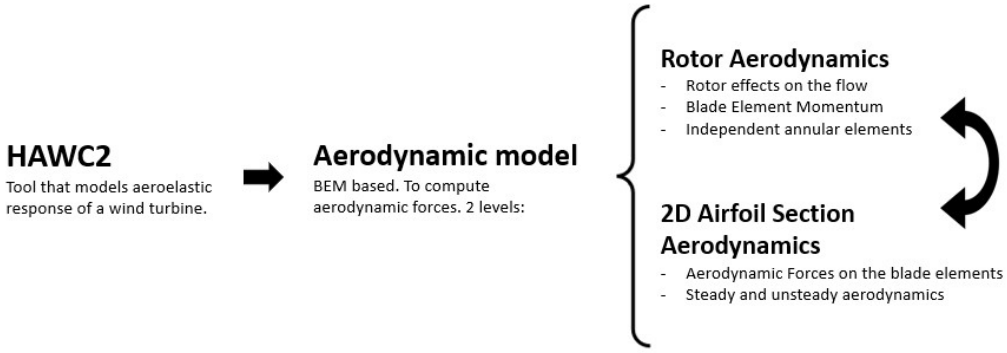

Figure 2.4: Visual scheme of HAWC2's aerodynamic model.

The first level takes into account that the rotor slows the air flow by capturing its energy. This is an effect called induction, where the flow approaching the rotor is modified in speed and direction by the presence of the rotor itself. The rotor aerodynamic is modelled with a Blade Element Momentum approach, which assumes that the wind turbine rotor can be modelled as an ideal rotor. The BEM model discretizes the area swept by the rotor into independent concentric annular blade elements. Computing the aerodynamic forces on each blade element is simplified to a 2D problem. The problem is solved using engineering models with low computational requirements for 2D Airfoil Section aerodynamics, as explained by the second level. The dynamics of the lift and drag forces are represented by the 2D Airfoil Section model, taking into account the rotor aerodynamic effects previously mentioned [28].

The two levels of the aerodynamic model are tightly linked to one another. To compute the aerodynamic forces on the airfoil section of a blade element, the speed and direction of the flow seen by the blade section needs to be known. The wind field, the motion of the structure, and the induction effects from the rotor aerodynamics will all have an impact on the flow seen by the blade section. The aerodynamic forces acting on the structure have an influence on its motion. In addition, the induction effects over the rotor depend on the wind field and the aerodynamic forces operating on the rotor area, resulting in a significant interaction among the various levels of the aerodynamic model [28].

2.3.3 Structural and cross-sectional model

The flexible multibody dynamics explains how the structure is modelled in HAWC2, also referred to as floating frame of reference [29]. A multibody formulation couples different independent bodies together using algebraic constraints. Each body is divided into a set of Timoshenko beam elements with six degrees of freedom to allow for flexibility. This implies that flapwise, edgewise, and torsional flexibility are taken into consideration

in the context of a blade. The main bodies serve as the framework of the structure. They ensure that every translation and rotation with respect to one another is taken into account. The Timoshenko beam elements add the effect of flexibility to each body. Beam elements have stiffness, mass and inertia, properties that are constant over each Timoshenko beam element [29]. If the beam properties are well defined, the dynamics of a flexible multibody simulation are fairly precise and useful for load analyses.

Figure 2.5 taken from reference [29] shows a graphical representation of how the blade structure is modelled in HAWC2. Beams are one dimensional: they only have a length, no width nor height. This beam model serves as a simple representation of a wind turbine blade.

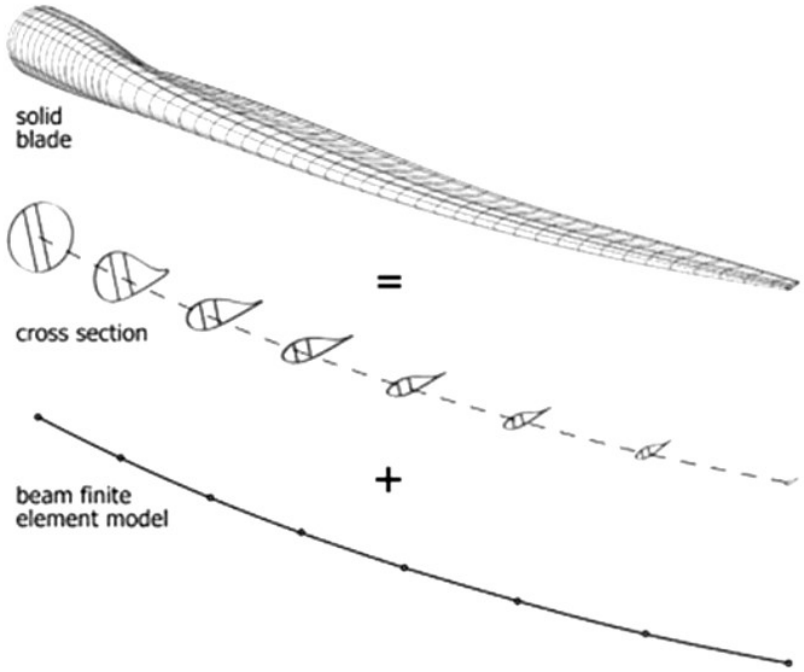

Figure 2.5: Wind turbine blade structure modelled in HAWC2. Figure taken from reference [29].

The top figure shows a 3D FE blade modelled with a large amount of elements, where the stiffness properties are defined by the material properties and a detailed description of the geometry. For an aeroelastic simulation, it would be too computationally costly. The middle and bottom figures show a beam model, which is less computationally heavy and employed by HAWC2. The complex blade geometry is simplified to a single line for a beam model, along which the stiffness, mass, and inertia properties of various cross-sections must be specified. As a result, the structural cross-sectional parameters must be known in advance, as HAWC2 does not support the analysis of generating cross-sectional parameters.

The BECAS software (which stands for Beam Cross section Analysis Software) is used to determine the cross-sectional stiffness and mass properties of a beam cross section in the aeroelastic tool HAWC2 [30]. This 2D finite element software computes the cross-section stiffness matrix, a 6x6 matrix that relates, for linear elastic beams, the cross-sectional forces and moments with the strains and curvatures.

It is important to be aware that each beam element is modelled as isotropic, which means that structural parameters are constant over one single beam element. The isotropic

approach of computing cross-sectional stiffness will be considered for ease of simplicity. The following constitutive relation (see equation 2.1) can define the blade modelled as an isotropic beam element, taken from reference [2]. This is the reason why the constitutive matrix has only diagonal terms. The left-hand side corresponds to the cross-sectional forces and moments, and the right-hand side represents the strains and curvatures. To model isotropic beam elements for a simple cross-section the following parameters (Table 2.1) are needed by HAWC2.

$$\begin{pmatrix} F_x \\ F_y \\ F_z \\ M_x \\ M_y \\ M_z \end{pmatrix} = \begin{pmatrix} GA \cdot k_x & 0 & 0 & 0 & 0 & 0 \\ 0 & GA \cdot k_y & 0 & 0 & 0 & 0 \\ 0 & 0 & AE & 0 & 0 & 0 \\ 0 & 0 & 0 & EI_x & 0 & 0 \\ 0 & 0 & 0 & 0 & EI_y & 0 \\ 0 & 0 & 0 & 0 & 0 & GJ \end{pmatrix} \cdot \begin{pmatrix} \gamma_x \\ \gamma_y \\ \gamma_z \\ \kappa_x \\ \kappa_y \\ \kappa_z \end{pmatrix} \tag{2.1}$$

The diagonal terms included in the constitutive matrix are:

- GAk_x: Shear stiffness in the x direction.
- GAk_y: Shear stiffness in the y direction.
- AE: Axial stiffness.
- EI_x: Bending stiffness about the x axis.
- EI_y: Bending stiffness about the y axis.
- GJ: Torsional stiffness.

Table 2.1: Cross-section properties needed in HAWC2.

Parameter	Definition	Unit
r	Point of the blade where the section starts	m
m	Mass per unit length	kg/m
xm	X-coordinate of the mass center	m
ym	Y-coordinate of the mass center	m
rix	Radius of gyration in x	m
riy	Radius of gyration in y	m
xs	X-coordinate of the shear center	m
ys	Y-coordinate of the shear center	m
E	Modulus of elasticity	N/m^2
G	Shear modulus of elasticity	N/m^2
I_x	Area moment of inertia in x	m^4
I_y	Area moment of inertia in y	m^4
J	Torsional stiffness constant	-
k_x	Shear factor in x	-
k_y	Shear factor in y	-
A	Cross-sectional area	m^2
θ_z	Structural pitch	degrees
xe	X-coordinate of center of elasticity	m
ye	Y-coordinate of center of elasticity	m

For wind turbine blades, the longitudinal stiffness often has little impact on simulation results. In addition, a wind turbine cross section has the flapwise bending stiffness (about

the horizontal x-axis) and the edgewise bending stiffness (about the vertical y-axis). The two caps of a blade are the ones that provide the main part of the flapwise bending stiffness. It is important to position the caps as separate from each other as possible, as the flapwise bending stiffness scales with the square of the distance between the caps. Sufficient flapwise bending stiffness is important to prevent the blades from crashing into the tower. Moreover, the torsional stiffness is an important parameter for wind turbine blades, as a twisting deformation changes the aerodynamic angle of attack and, therefore influences the aerodynamic forces. Furthermore, shear webs are added to wind turbine blades to provide enough shear stiffness. As previously mentioned, HAWC2 uses the Timoshenko beam theory, which describes the lateral deformation of a beam based on both bending and shear stiffness. When a shear web couples the two caps together, the deformation of the blade is reduced [31]. Figure in Section shows the basic elements of a wind turbine blade section.

2.4 3D FE model

On the other hand, ABAQUS is a 3D finite element simulation software used to compute structural performance of wind turbine blades. In this case, a 3D section of a wind turbine blade is modelled in ABAQUS to compute high-fidelity structural properties.

To describe the mechanical behaviour of wind turbine blades, HAWC2 relies on beam theory. As a result, inputs such as beam cross-section stiffness and mass properties are needed. Although the beam theory model assumptions used to calculate the cross-sectional stiffness properties of a wind turbine blade are sufficient for calculating aerodynamic loads, they fall short of what is required to analyse the structural performance of a blade when damaged due to exposure to extreme weather conditions.

For those purposes, a 3D blade section is modelled in ABAQUS to account for structural non-linearities associated with geometry and composite layup that are neglected in the beam theory model used by the aeroelastic tool. A 3D finite element modelling approach is used to compute stiffness properties of 3D blade sections and to conduct advanced progressive failure analysis, which enables precise composite failure and foam crushing prediction [32]. For this study, foam core crush will be analysed together with delamination of the unidirectional (UD) composite laminate. Foam core crush is in built model in ABAQUS, whereas delamination is obtained post calculation.

The input file for the 3D FE modelling of blade sections includes the mesh, the loading and boundary conditions, layup configuration, material properties, element type, and numerical settings, and will be further explained in Chapter 3, Section 3.2.

3 Modelling and simulation

The models used in the aeroelastic tool HAWC2 and the 3D FE software ABAQUS are described in the following chapter, respectively. First, the aeroelastic model is described, including the most relevant specifications of the wind turbine modelled in the study, the extreme wind profile modelling, and detailed explanations on how cross-sectional moments are transformed into rotation angles (needed to solve convergence issues, as will be explained). Subsequently, the 3D FE set-up is described, including the modelling of a 3D blade section, the components and material properties of the structure, the loading and boundary conditions, the numerical settings, and the computer environment. In addition, an explanation on how to calculate the stiffness properties from the 3D blade model is described, together with the failure analysis criterion employed to determine whether the blade section experiences composite failure or foam core crush.

3.1 Aeroelastic setup

3.1.1 Wind turbine specifications

The DTU 10MW Reference Wind Turbine has been selected as the wind turbine for this study. This section covers the most crucial aspects relevant to this study. For more details, please see the cited source [13].

The DTU 10MW Reference Wind Turbine has a cut in wind speed of 4 m/s and and a cut out wind speed of 25 m/s, as mentioned in Section 1.1. The wind turbine has three blades and a rotor diameter of 178.3 m, with a blade length of more than 80 m. Regarding the structural design, the blade has been divided in 51 sections across its length, and for each section the cross-sectional stiffness properties were calculated using the 2D finite element software BECAS. As mentioned in Section 2.3, the beam theory assumptions have been used, where the sections of the blade have been modelled as beam elements. The model is assumed as isotropic.

3.1.2 Wind profile modelling

One of the objectives for the blade behaviour prediction interface is to model an extreme wind profile in HAWC2 with data obtained from real wind measurements. To start with, the meaning of extreme wind profile needs to be defined. According to the Saffir–Simpson hurricane intensity scale [33], a wind profile with a sustained mean wind speed around 33 to 43 m/s is considered to be dangerous and produce potential damage. The modelled extreme wind profile will fulfill this characteristic, and in addition it will have a remarkable wind gust. This is a sudden, brief increase in the speed of the wind.

The next step is to find real wind data measurements that fulfill these specific requirements. In order to do so, the DTU's Database on Wind Characteristics [34] was consulted. This repository contains a turbulence measurement collection [35] which consists of time series of turbulence measurements. The measurements primarily include

wind speed and wind direction signals, and are primarily intended for wind turbine design. The collection contains a list of sites with documentation about the measurement setup and instrumentation. This list may be used as a help to find the appropriate measurement data before downloading.

The turbulence measurement collection was filtered to search for collections with extreme wind profiles. For the selected collections, to optimize the searching process a MATLAB code was developed to find a wind profile with the desired characteristics. The code unzips the downloaded collection, opens the files, and saves the maximum mean wind speed along with the sensor that measured the wind speed, and the location of the corresponding file.

After running the code, the time series of turbulence measurements that better fulfills the extreme wind profile requirements corresponds to data measurements from three tall met masts at Skipheya, on the Norwegian island of Frøya [36]. This dataset contains raw time series measurements of wind speed and direction as well as run statistics. The duration covers more than three years of observations starting in 1992. The data file corresponds to day 360 in the year 1992, and it is named by '1700_010.dat'. Sensor number 10 measurements are the ones that better represent an extreme wind profile, with a mean wind speed of 34.55 m/s and a local peak of 49.1 m/s, as seen in Figure 3.1. The sensor is placed at a height of 41m, and the time series has a duration of 3600 seconds and was sampled at a frequency of 0.85 Hz. The modelled wind profile has a remarkable wind gust and the mean wind speed value satisfies the specifications.

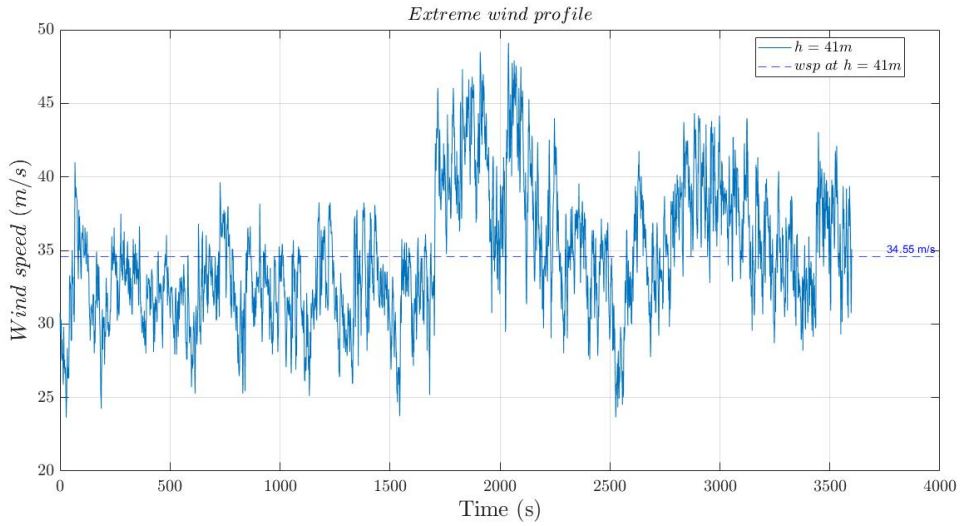

Figure 3.1: Extreme wind profile obtained from data file.

To model the chosen wind profile, HAWC2 requires the turbulence files of the three wind field components: u, v, and w. The turbulence component u is obtained by subtracting the mean wind speed from the file measurements, whereas the v and w components are calculated using *Turbgen*, a turbulence field generation and constrained turbulence simulation package.

The *Turbgen* package is part of the HiperSim software. Hipersim is a turbulence box generation tool available as a free Python package (pypi.org/hipersim). This tool was used in the Hiperwind project [37]. The turbulence-related functionalities of Hipersim are specially provided by the Turbgen module. The Turbgen module's main purpose is to produce wind fields complying to Mann's spectral tensor specification [38] using Mann's turbulence generation algorithm [26]. An additional function is to generate turbulence

boxes based on specified constraints, with the objective of specifying the exact values of the wind field at a list of points that shape the turbulence box. More information of the constrained simulation algorithm is provided in Dimitrov and Natajaran [39].

To create the turbulence files for the chosen wind profile, the last mentioned functionality is used. Using the Hipersim *Turbgen* tools, a constrained turbulence box can be simulated to recreate the flow structures seen in observations [37]. The turbulence box is generated by constraining a single component, which in this case is the u component, as it is the one obtained from the data file turbulence measurements. To calculate the dimensions of the turbulence box, the following initial parameters are needed:

- Mean wind speed at hub height, *wsp*.
- Standard deviation of the turbulence measurements, *std*.
- Turbulence intensity of the u component, *tint*, obtained dividing the standard deviation of the turbulence measurements by the mean wind speed.
- Duration of the time series, *time_sim*.

However, the selected data measurements correspond to a height of 41m, and HAWC2 models the wind profile at a height corresponding to the hub height. Since the main purpose of this project is the analysis of the blades behaviour under extreme wind conditions, it is sufficient to translate the wind profile from the data measurements to hub height, but taking into account the wind shear effects. Using the power law shear definition (3.1) with an α coefficient equal to 0.3, the mean wind speed at hub height $U(z_{ref})$ can be computed knowing the mean wind speed at the sensor height $U(z)$. The α exponent is an empirically calculated coefficient that changes with atmospheric stability.

$$U(z) = U(z_{ref}) \left(\frac{z}{z_{ref}} \right)^{\alpha} \tag{3.1}$$

The initial parameters used to generate the turbulence box are summarized in the following table (Table 3.1), obtained from the extreme wind profile "1700_010.dat" file.

Table 3.1: Initial parameters to calculate the dimensions of the turbulence box.

Initial parameters	*wsp*	*std*	*tint*	*time_sim*
Value	47.683 m/s	4.390	0.092	3600 s

The dimensions of the turbulence box are calculated manually to match the specifications of the wind turbine. The turbulence box dimensions are represented with Lx, Ly, and Lz, as shown in Figure 3.2, taken from reference [3]. The length of the turbulence box Lx should correspond to the simulation time to store all the wind profile information during that time, and it is computed as the duration of the time series multiplied by the mean wind speed during that time. Ly and Lz are computed manually and correspond to the ones that make the centre of the wind turbine to match the grid points of the turbulence box to increase the method's accuracy. Important to take into account that the turbulence box should cover the entire wind turbine rotor, so the cross-section dimensions should be higher than the diameter swept by the wind turbine blades, as shown in Figure 3.3, modified based on reference [40]. The turbulence box is located at a height of 20 m above the ground, and its centre coincides with the centre of the wind turbine. The computed values are shown in Table 3.2.

Table 3.2: Dimensions of the turbulence box.

Lx (m)	Ly (m)	Lz (m)
171658.800	206.667	206.667

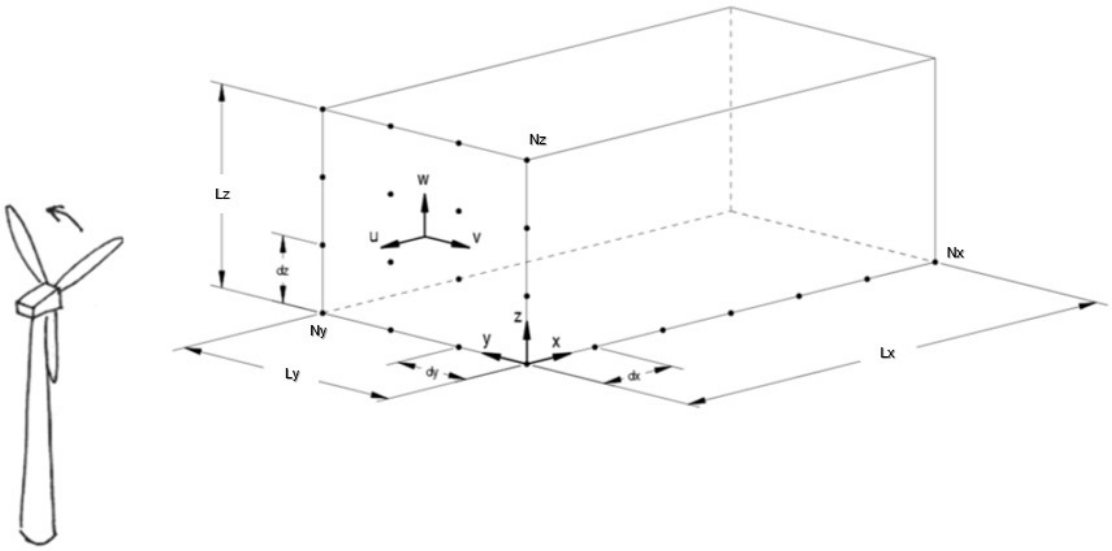

Figure 3.2: Dimensions of the turbulence box. Figure taken from reference [3].

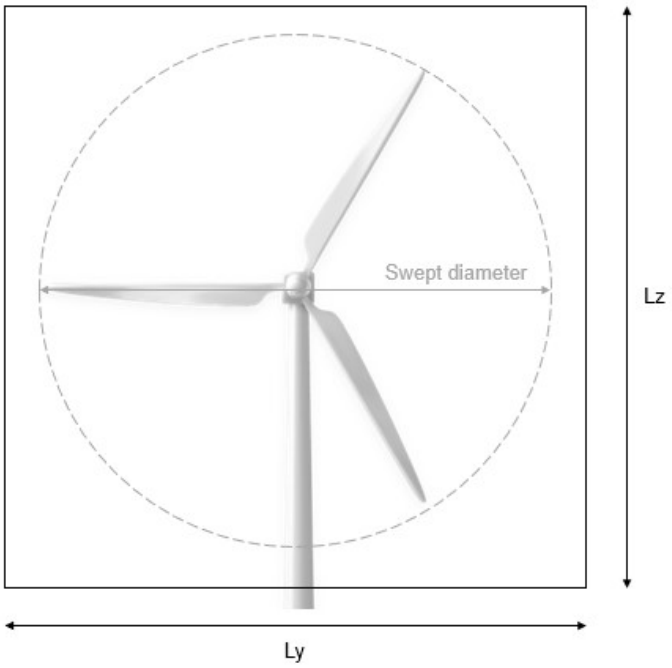

Figure 3.3: Turbulence box front view. Figure adapted from [40].

Once the dimensions of the turbulence box are known, the turbulence field parameters can be defined with the values shown in Table 3.3, and the unconstrained turbulence field can be generated. In the list of symbols, the definitions of the parameters and their units are provided. Regarding the high frequency compensation parameter (HighFreqComp), it determines if the turbulence generation is subject to high frequency compensation as

stated in [26]. The values corresponding to dx, dy, and dz are calculated with equations 3.2, 3.3, and 3.4 respectively.

Table 3.3: Turbulence box generation parameters (see List of Symbols 1).

Parameters	**Value**
Nx	4096
Ny	32 (default)
Nz	32 (default)
dx	41.91
dy	6.66
dz	6.66
L	29.4 (default)
Γ	3.9 (default)
$\alpha\epsilon$	0.1
HighFreqComp	1
Seed number	10

$$dx = \frac{Lx}{Nx} \tag{3.2}$$

$$dy = \frac{Ly}{Ny - 1} \tag{3.3}$$

$$dz = \frac{Lz}{Nz - 1} \tag{3.4}$$

To constrain the turbulence field, constraint arrays need to be specified in the directions of the turbulence box (x,y,z) and in the u direction of the wind. The x constraint array has a length corresponding to Lx, the y constraint array specifies the middle of the turbulence box, and the z constraint array specifies the height at which the turbulence field will be generated. The component u constraint is applied at the hub height, and it is an array with the turbulence measurements obtained in the "1700_010.dat" file. Constraints are applied and the new constrained turbulence field is generated, obtaining modified, constrained wind field components u, v and w, as can be seen in Figure 3.4.

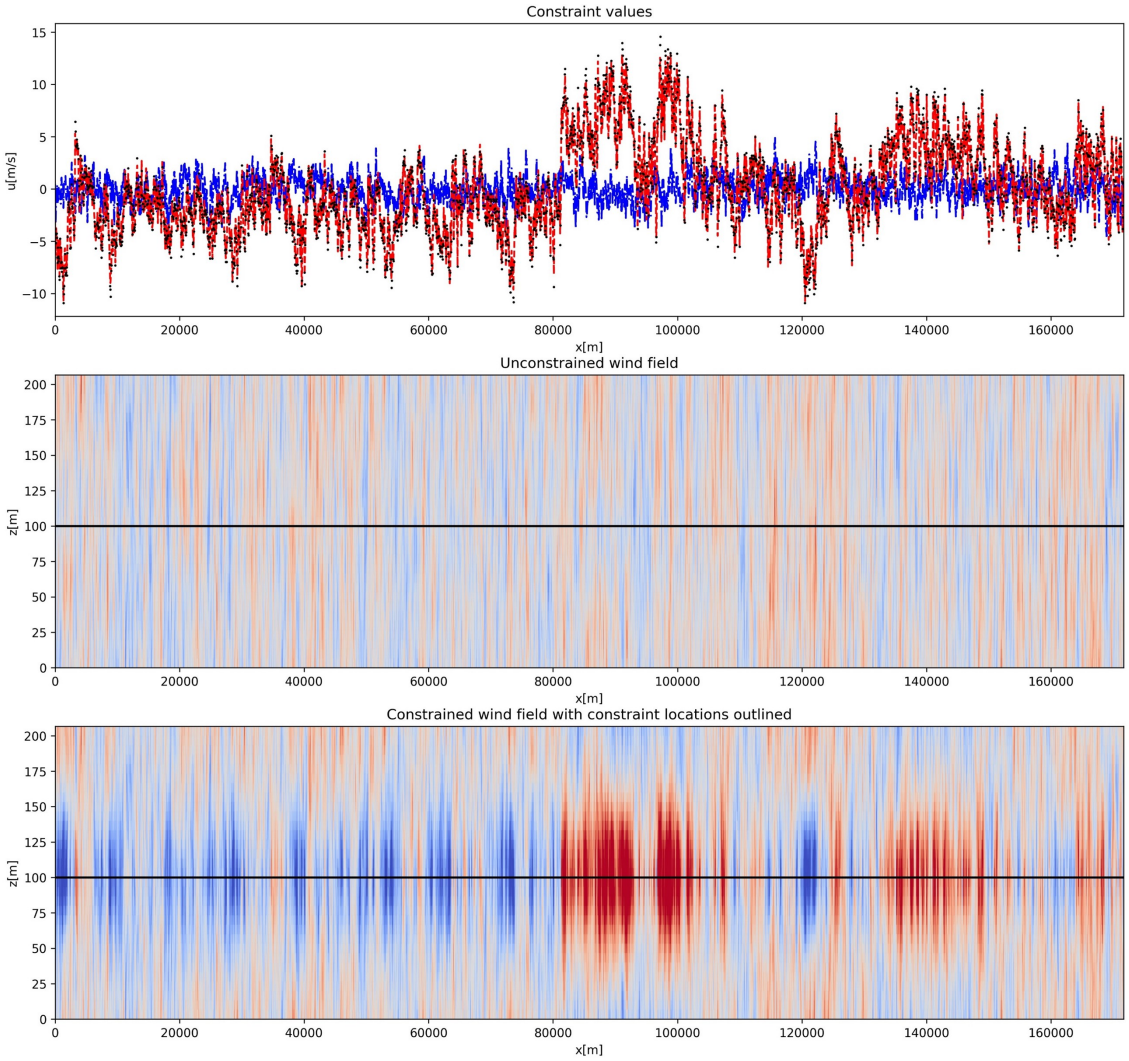

Figure 3.4: Constrained wind field. Top plot: Blue curve shows the time series of a turbulence field at the centre of the turbulence box before the application of constraints. Black curve shows the required constraint. Red curve shows the time series of the turbulence field after the application of the constraint. Middle plot: a cross-section of the unconstrained field is shown, in the x-z plane at the middle position in y. Black line indicates where the constraint is applied (at the middle position in z. Bottom plot: shows a cross-section of the turbulence field in the x-z plane after the application of the constraint in the u component. The location with higher wind speed that meets the constraint requirements is highlighted in red with a stronger shading.

Now that the three wind field components are defined, they can be extracted as turbulence files and used in the aeroelastic tool to model the wind profile. The following figure (Figure 3.5) shows a comparison between the wind measurements from the "1700_010.dat" file (blue curve) and the wind profile generated by HAWC2 (red curve). It can be seen that the turbulence pattern in both profiles is practically the same, measured with the standard deviation of the wind profile, and that the mean wind speed is the only difference. This is due to the fact that the wind profile has been shifted upwards to model it at hub height, as explained above. Table 3.4 shows the values of standard deviation of both wind profiles, which are really close to each other. Note that the parameter Nx in Table 3.3 has a value of 4096, when normally a value of 8092 is used for 10 minute wind speed time series. However, this did not affect the resolution of the wind profile.

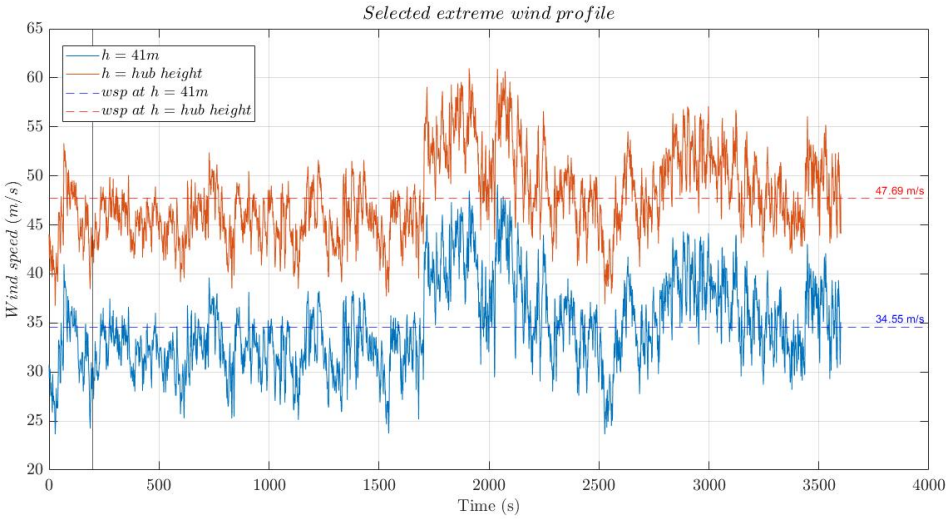

Figure 3.5: Comparison between real data wind profile (blue curve) and wind profile modelled in HAWC2 (red curve).

Table 3.4: Standard deviation of the real data wind profile (h = 41m) and wind profile modelled in HAWC2 (h = hub height).

	(h = 41 m)	**(h = Hub height)**
Standard deviation, std	4.390	4.079

As mentioned in Section 2.2, with a wind profile with these magnitudes, the order of magnitude of the cross-sectional forces and moments correspond to the ones reflected in Table 3.5.

Table 3.5: Order of magnitude of the cross-sectional forces under an extreme wind profile.

Forces, N (F_x, F_y, F_z)	**Torsional moment, Nm** (M_z)	**Bending moments, Nm** (M_x, M_y)
$\approx 10^4$	$\approx 10^4$	$\approx 10^5$

3.1.3 Conversion of moments to rotational displacements

As a extremely complex and detailed 3D blade section has been modelled in a 3D FE software, in order to avoid convergence issues the cross-sectional moments obtained with the aeroelastic tool are converted into rotational displacements. For this purpose, the beam theory has been used. The blade section can be modelled as a beam with a bending moment applied at both ends. Two bending moments are applied in the blade section, the flapwise bending moment (moment in the x direction) and the edgewise bending moment (moment in the y direction) as shown in Figure 2.3. First, the flapwise moment will be applied and the rotation angle in the x direction, θ_x, will be obtained, and then the edgewise moment will be applied to compute the rotation in the y direction, θ_y. The same procedure will be used for both bending moments.

To compute the rotation angle due to the presence of a bending moment, the curvature κ is first to be obtained. The curvature is defined as the bending moment at the end of the beam divided by the bending stiffness, as shown in equation 3.5. The same equation is

used for both the bending moment in the x direction and for the bending moment in the y direction, with its respective moments of inertia. The bending stiffness (equation 2.1) are inputs already defined in the aeroelastic tool, as previously mentioned.

$$\kappa = \frac{M}{E\ I} \tag{3.5}$$

The curvature κ is known to be the reciprocal of the radius of curvature R, as shown in equation 3.6.

$$R = \frac{1}{\kappa} \tag{3.6}$$

By means of trigonometric relations, the rotation angle θ can be obtained as shown in Figure 3.6 and following equations 3.7, 3.8, and 3.9. δ is the displacement of the end of the deformed beam with respect to its undeformed position, in meters, and L_{sec} is the length of the blade section, in meters.

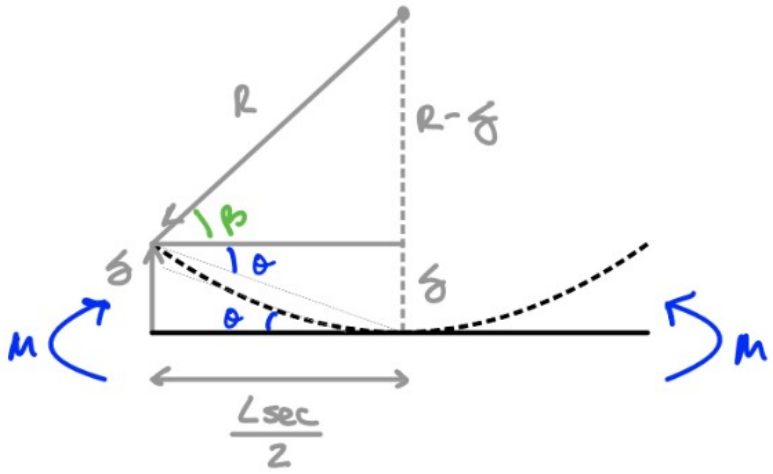

Figure 3.6: Calculation of the rotation angle.

$$\beta = \arccos(\frac{L_{sec}/2}{R}) \tag{3.7}$$

$$\delta = R\ (1 - \sin(\beta)) \tag{3.8}$$

$$\theta = \arctan(\frac{\delta}{L_{sec}/2}) \tag{3.9}$$

Important to highlight that both θ_x and θ_y are expressed in radians, as the 3D FE software needs to receive rotational displacement in radian units.

3.2 3D FE model set-up

3.2.1 Components and material properties

The 3D blade section that has been used for this study is the same as the one used in Miao & Chen [32], and has been modelled according to the DTU 10MW Reference Wind Turbine structural design [13]. The blade is made from glass fiber reinforced composites and sandwich structures with foam core material. The composite layup of the blade is described in terms of a stacking-sequence of layers that represented multidirectional plies.

Figure 3.7 shows the components of a wind turbine blade section, based on reference [4]. It consists of two leading edge panels, two tailing edge panels, and two spar caps separated by two shear webs. Section 2.3.3 explained the main functionality of the components. It also shows the materials of which the 3D blade section is made. The most relevant materials for this study are the unidirectional composite materials and the foam core inside the sandwich structures (shear webs, and leading and trailing edge panels). Foam core is found in the shear webs and the leading edge and trailing edge panels. Unidirectional composite material is found in the spar caps, biaxial in shear webs and triaxial all around the blade section.

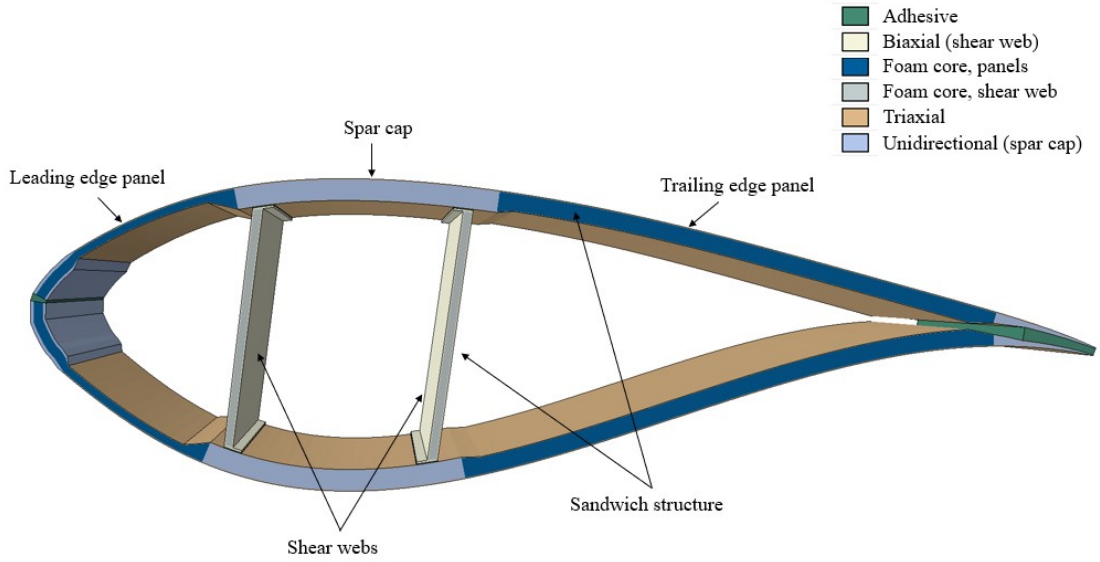

Figure 3.7: Components and materials of the 3D wind turbine blade section. Figure based on reference [4].

The elastic properties of the composite material are displayed in Table 3.6, Table 3.7, and Table 3.8, all taken from reference [32]. For the foam core inside the sandwich structures, a PVC foam Divinycell H45 material was used, with the material properties displayed in Table 3.9.

Table 3.6: Young's modulus of the composite material in the 3D blade section. Table taken from reference [32].

Materials	**Young's modulus (GPa)**		
	E_{11}	E_{22}	E_{33}
Unidirectional (0°)	39.00	13.00	13.00
Biaxial (±45°)	12.50	12.50	12.50
Triaxial (0°/±45°/90°)	17.80	13.05	13.05

Table 3.7: Shear modulus of the composite material in the 3D blade section. Table taken from reference [32].

Materials	**Shear modulus (GPa)**		
	G_{12}	G_{13}	G_{23}
Unidirectional (0°)	3.40	3.40	3.40
Biaxial (±45°)	10.30	10.30	10.30
Triaxial (0°/±45°/90°)	9.10	9.10	9.10

Table 3.8: Poisson's ratio of the composite material in the 3D blade section. Table taken from reference [32].

Materials	**Poisson's ratio**		
	ν_{12}	ν_{13}	ν_{23}
Unidirectional (0°)	0.205	0.205	0.350
Biaxial (±45°)	0.498	0.498	0.498
Triaxial (0°/±45°/90°)	0.472	0.472	0.472

Table 3.9: Material properties of PVC foam core material.

Material ρ / $kg\ m^3$	Young's Modulus E / MPa	Poisson's ratio ν	Yield strength σ_c^0 / MPa	Yield stress ratio k
45	30.0	0.3	0.5	1.0

3.2.2 Geometric model and numerical set-up

The blade section modelled in the 3D FE software ABAQUS is 1 m long. The length has been modified with respect to the blade section used in Miao & Chen [32] because in the aeroelastic tool HAWC2 the blade sections are approximately 1 m long. Finite element mesh details are shown in Figure 3.8. The 3D blade model employs solid components of the C3DR8 element type. Typical mesh sizes range from 25 × 38 × t mm for solid elements at sandwich panels to 25 × 27 × t mm for spar cap regions and 25 × 8 × t mm for trailing edge bondlines, where t denotes the range of material thicknesses. Mesh sensitivity studies were done in [32] to determine the mesh size.

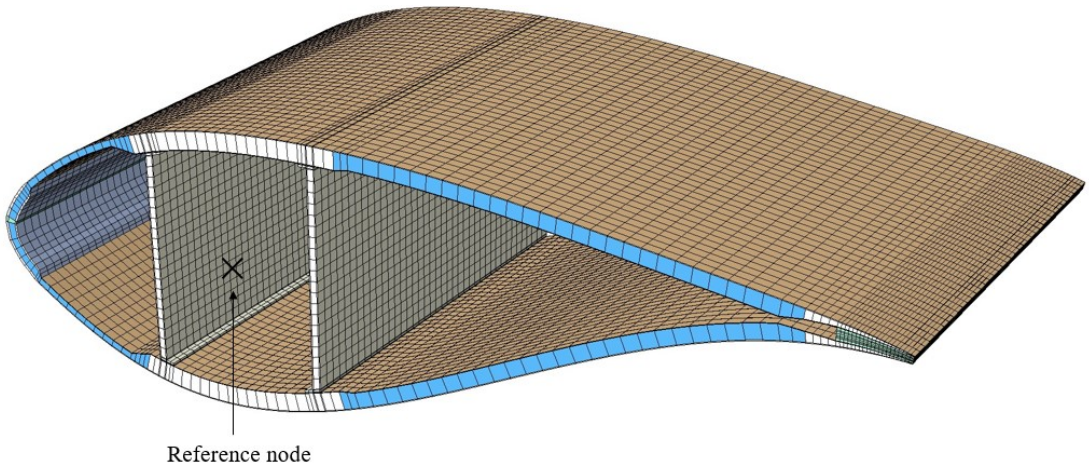

Figure 3.8: Mesh details and reference node (marked with an x).

Two different types of simulations are conducted in this study. The dynamic option is conducted to model the blade section under the dynamic loading conditions obtained from the aeroelastic tool HAWC2, whereas the stiffness properties are computed under static loading conditions. The dynamic option is frequently used for nonlinear applications and allows for direct integration of a dynamic displacement response in ABAQUS. However, instabilities caused by the structure's nonlinear response challenge convergence. The following numerical settings are made to improve the convergence [41]:

- Cross-sectional bending moments are converted into rotational displacement.
- The initial time increment for the dynamic step is set to $1 \times 10^{-}6$. The minimum time increment is set to $1 \times 10^{-}13$ and the maximum to 0.5. The dynamic option is often used for nonlinear applications and provides direct integration of a dynamic displacement response in Abaqus studies [41].
- The NOHAF parameter is employed to disable the computation of half-increment residuals and so avoid certain accuracy checks for the automated time incrementation system.
- The APPLICATION=TRANSIENT FIDELITY parameter is predetermined as the default approach for issues in the model without contact to select a method for an accurate solution with minimal numerical damping.
- The TIME INTEGRATOR=HHT-TF parameter is configured to use the Hilber-Hughes-Taylor time integrator with default parameter values that offer little numerical damping. This is the default for APPLICATION=TRANSIENT FIDELITY.
- The SINGULAR MASS=ERROR parameter is used to display an error message and cease operation if a singular global mass matrix is found while computing the velocity and acceleration adjustments.

The static simulation is conducted to compute the stiffness properties of the 3D blade section. To avoid convergence issues, the following numerical settings are used [41]:

- The initial time increment for the static step is set to $1 \times 10^{-}6$. The minimum time increment is set to $1 \times 10^{-}10$ and the maximum to 0.05.
- The STABILIZE parameter is used to activate automatic stabilization, to avoid sudden buckling or collapse without materially changing behavior while the issue remains stable.

In addition, two additional parameters inside the control option are defined in the step set-up to obtain a solution in case extreme nonlinearities occur. It helps in obtaining a more efficient solution [41].

- The ANALYSIS=DISCONTINUOUS parameter is used to increase performance for highly discontinuous behavior by permitting a large number of iterations before starting any convergence rate checks.
- The PARAMETERS=FIELD parameter is employed to provide conditions that fulfill a field equation. In this situation, the field for which the parameters are being given can be defined by this parameter.
- The PARAMETERS=TIME INCREMENTATION is configured to establish the settings for time increment control.

To simulate foam core crush failure in the blade structure, the foam core is modelled as a crushable material based on a phenomenological constitutive relation. The development of the yield surface is determined by isotropic hardening [32].

3.2.3 Loading and boundary conditions

A rigid body reference node, indicated by an x mark in Figure 3.8 is set in the blade section in order to concentrate all the loads applied in the respective section. The two ends are clamped, and the reference node is allocated a local coordinate system and positioned at the elastic center.

For the dynamic analysis, rotational displacements in both the x and y directions are applied on the reference nodes, simulating the effects of flapwise and edgewise moments respectively. In addition, the boundary conditions are set to allow rotation in both x and y direction.

For the static analysis, different loading and boundary conditions are applied. The stiffness properties of the 3D blade section are computed by running six different simulations. Forces and moments applied in the three directions are applied independently to the blade structure. The boundary conditions involve fixing one of the sections of the blade and applying the force or moment in the reference node in the free section of the blade, allowing movement just in the direction of the force or moment.

3.2.4 Computer information

The simulations are performed on the ABAQUS DTU Cluster [42] with E5-2640 v3, 8 cores processor, 2.6-3.4GHz, and 128 GB installed RAM.

3.2.5 Update of stiffness properties

If damage is induced in the blade section, the stiffness properties will be recalculated for the blade structure with the 3D FE software ABAQUS, and the interface will update them into the aeroelastic tool HAWC2 for the next calculation of aerodynamic loads.

As described in Section 2.3.3, the cross-sectional stiffness properties of the blade are computed using BECAS (BEam Cross section Analysis Software), a 2D finite element based approach. However, the initial stiffness parameters established in the aeroelastic tool will be recalculated with the 3D FE program to ensure that the ones employed by the aeroelastic tool and those acquired with the 3D FE software are the same.

To calculate the diagonal terms, the constitutive relation representing the stiffness matrix mentioned in Section 2.3.3 is used (shown in equation 2.1). Each cross-sectional force and moment will be applied independently in the 3D blade section, as described in Section 3.2.2. As a result, displacements and rotational displacement are obtained in the 3D FE simulation. Strains and curvatures in the x, y, and z directions are computed, and with equations 3.10, 3.11, 3.12, 3.13, 3.14, and 3.15 the stiffness properties of the 3D blade section are obtained.

$$GAk_x = \frac{F_x}{\gamma_x} \tag{3.10}$$

$$GAk_y = \frac{F_y}{\gamma_y} \tag{3.11}$$

$$AE = \frac{F_z}{\epsilon_z} \tag{3.12}$$

$$EI_x = \frac{M_x}{\kappa_x} \tag{3.13}$$

$$EI_y = \frac{M_y}{\kappa_y} \tag{3.14}$$

$$GJ = \frac{M_z}{\kappa_z} \tag{3.15}$$

To obtain the elastic modulus E and the shear modulus G, the system of equations defined by stiffness matrix shown in the previously indicated equation 2.1 is solved. The cross-sectional area A together with the shear factors k_x and k_y are already known, since they depend on the geometry of the structure. Once E and G are known, the stiffness properties are updated in the aeroelastic tool HAWC2 so that the following aerodynamic loads can be computed accordingly.

3.2.6 Blade failure analysis

The composites, foam core and adhesive materials can fail during the loading [32]. The blade structure is subject to bending moments in both the x and y directions, and the main component that is responsible for supporting these loads are the spar caps, which are coupled together by the shear webs. The spar caps are the ones that provide the most of bending stiffness to the structure. In this work, the delamination of the unidirectional (UD) composite laminate and foam core crushing are evaluated. To evaluate the failure in the UD composite laminate, the maximum strain failure criterion will be employed. On the other hand, the foam core crush failure will also be evaluated in the sandwich structures. Figure 3.9 shows which materials are prone to failure under the above mentioned loading conditions, and their location in the blade section structure.

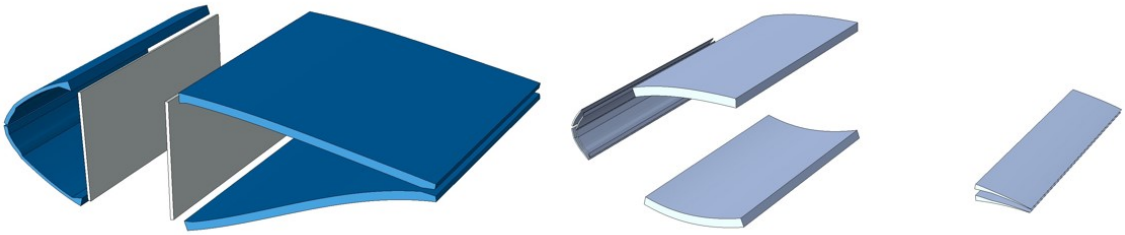

Figure 3.9: Materials that can fail during the loading. Figure on the left: Foam core of the sandwich structures. Figure on the right: Unidirectional laminate.

The maximum strain failure criterion is employed to detect delamination of the UD material. If the strains of the material are higher than the ultimate strains shown in Table 3.10, the UD material experiences delamination. The table is taken from reference [32].

Table 3.10: Ultimate strain components of composite materials (unit: mm mm^{-1}). Table taken from reference [32].

Materials	$\epsilon_{33}^{u,t}$	ϵ_{13}^{u}	ϵ_{23}^{u}
Unidirectional (0°)	0.0021	0.0110	0.0081
Biaxial (±45°)	0.0122	0.0122	0.0135
Triaxial (0°/±45°/90°)	0.0122	0.0122	0.0135

Due to the production process, anisotropy in foam core materials is usual. Foam core materials with higher density exhibit greater anisotropy than those with lower density. The foam core material used in this study has a nominal density of 45 kg m^3, lower than 1000 kg m^3, so it can be treated as isotropic in the simulations as its anisotropy is not significant [32].

4 Results and discussion

Several case studies have been conducted to test the performance of the developed interface. A perfect new blade is assumed in Case study 1 and Case study 2. For Case study 1 the aerodynamic loads corresponding to the extreme wind profile modelled in Section 3.1.2 are applied to the 3D FE blade section. A sensitivity analysis is then carried out to find the minimum rotational displacements values in both x and y directions that induce damage to the blade structure. Case study 2 reflects the situation where the blade structure is subject to a wind profile that produces the minimum rotational displacement to induce damage to the blade structure. Finally, for both Case study 3 and Case study 4 the foam core material used in the sandwich structures has been changed to another with lower mechanical properties than the ones used in the initial design of the blade structure, and the wind profiles used for Case study 1 and 2 will be applied again to the modified blade structure.

4.1 Case study 1

In the following case study the extreme wind profile modelled in Section 3.1.2 is applied to the wind turbine. Of the total duration of 3600 s, 50 s corresponding to the peak zone of the wind profile will be used for the 3D FE simulation. The obtained cross-sectional moments are converted to rotational displacements with the procedure explained in Section 3.1.3, obtaining the values shown in Figure 4.1 and Figure 4.2.

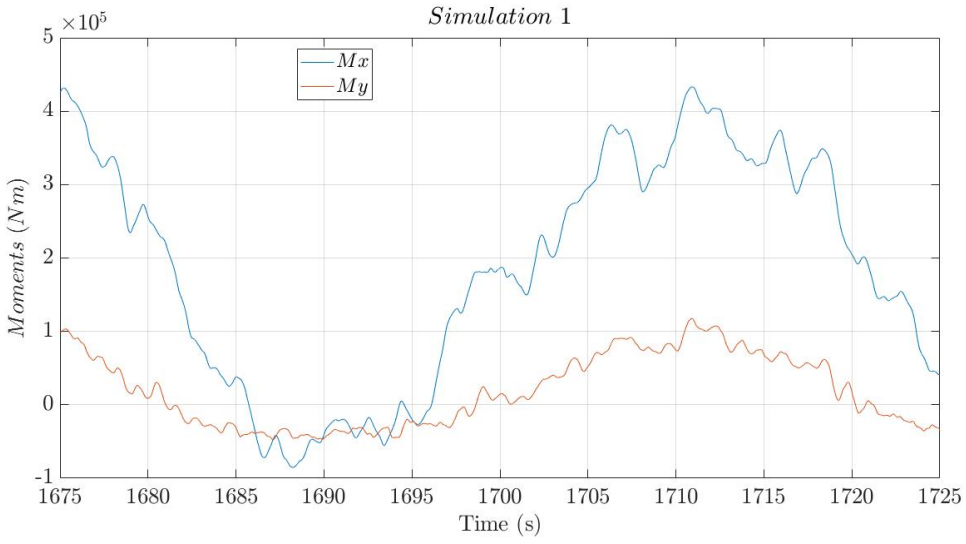

Figure 4.1: Case study 1. Cross-sectional bending moments in the peak zone of the modelled extreme wind profile.

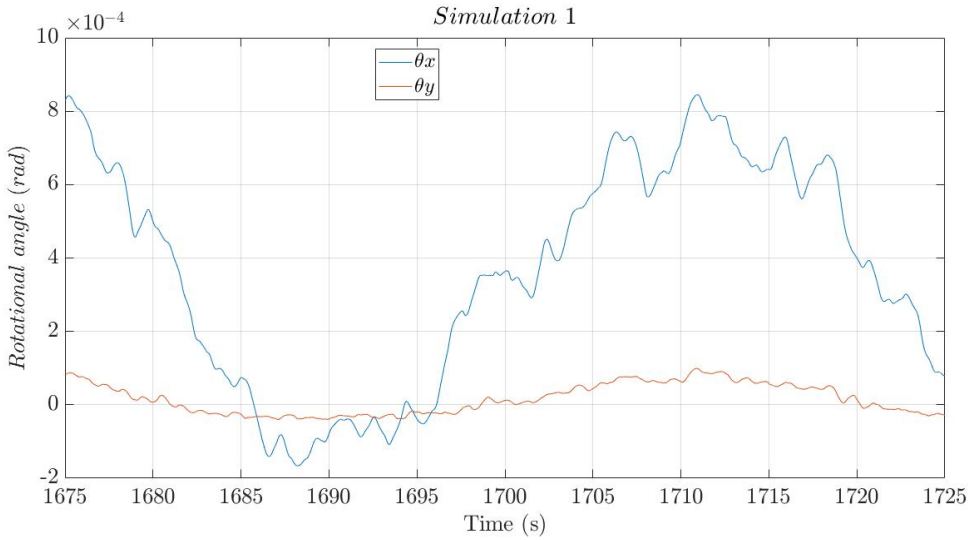

Figure 4.2: Case study 1. Rotational displacements corresponding to the bending moments in the peak zone of the modelled extreme wind profile.

The total time of the 3D FE simulation is of 60 sec, counting with 10 additional seconds to unload the structure, as the stiffness properties need to be computed in the unloaded structure. However, no damage is induced in the blade structure with the designed extreme wind profile, so an update of the stiffness properties of the blade structure is not considered for this case study. Failure analysis is performed to the blade structure, where Figure 4.3 shows that there is no plastic deformation on the foam core material. Delamination of the unidirectional composite material does not occur either, as shown in Table 4.1, since the maximum strains in the specified directions are lower than the ultimate strains.

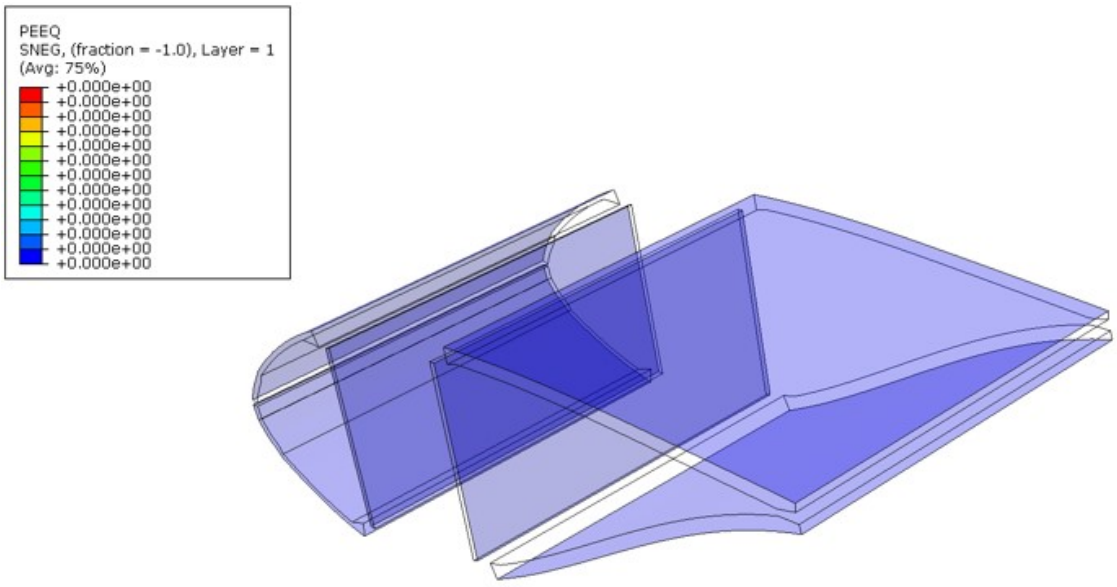

Figure 4.3: Case study 1. No plastic deformation in the foam core material of the blade structure.

Table 4.1: Case study 1. Check for delamination in the UD composite material.

UD composite material	ϵ_{33}	ϵ_{13}	ϵ_{23}
Ultimate strain	2.100e-03	1.100e-02	8.100e-03
Simulation max. strain	1.658e-04	2.761e-04	8.037e-05

Even though an extreme wind profile was applied to the blade structure, no damage has been induced. This justifies the good design of the blade structure and an appropriate selection of materials. A perfect new blade is assumed in this study, and fatigue loads, manufacturing flaws or blade degradation is not considered.

4.2 Sensitivity study

A sensitivity study is carried out to find the values of rotational displacement in x and y direction to induce damage in the blade structure. Static analysis are performed and the following results are obtained (Table 4.2). A value of 0.0055 radians for the rotational displacement in the x direction, θ_x, is the minimum value for which the blade structure experiences foam core crush, this is plastic deformation in the foam core material in the sandwich structures. On the other hand, the minimum rotational displacement in the y direction, θ_y, is 0.002 radians in order for the blade structure to experience foam core failure (Table 4.3).

Table 4.2: Minimum value of rotational displacement in the x direction, θ_x, to induce damage in the blade section.

θ_x	**Foam core crush**	**Delamination UD composite**
0.005	No	Yes (just ϵ_{33})
0.0055	Yes	Yes (just ϵ_{33})

Table 4.3: Minimum value of rotational displacement in the y direction, θ_y, to induce damage in the blade section.

θ_y	**Foam core crush**	**Delamination UD composite**
0.001	No	No
0.002	Yes	Yes (just ϵ_{33})

4.3 Case study 2

Knowing the minimum values at which the blade structure experiences permanent damage, a different wind profile will be modelled in order to reach at least those values and thus induce damage to the structure. The new wind profile is shown in Figure 4.4. This new extreme wind profile has a mean wind speed of 80 m/s, a turbulence intensity of 0.055, and a total duration of 1500 s. The peak zone is the one to be used in the 3D FE simulation, following the same approach as in Case study 1. Of the total duration, 50 s corresponding to the peak zone will be used for the dynamic simulation. By increasing the mean wind speed to 80 m/s and using a lower turbulence intensity with respect to the modelled extreme wind profile, higher bending moments in the x direction are obtained in the new extreme wind profile.

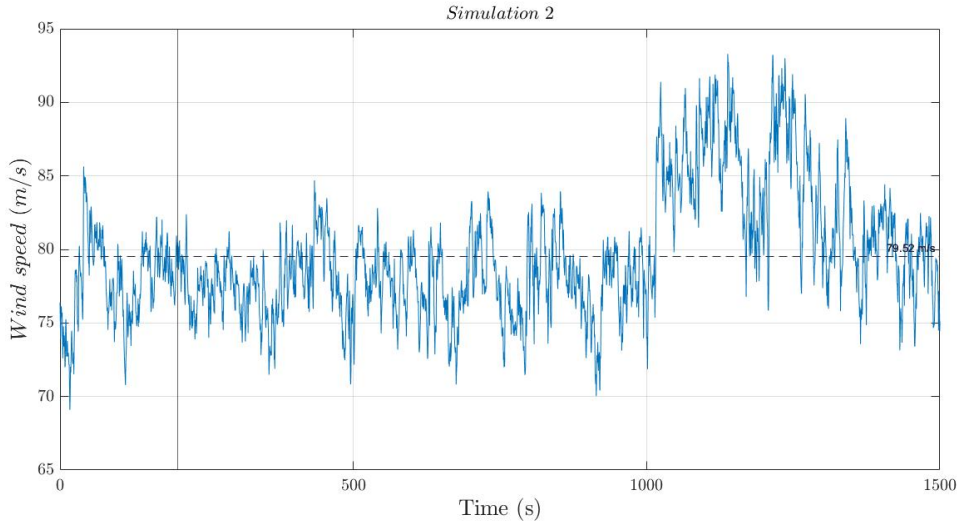

Figure 4.4: Case study 2. Extreme wind profile with a mean wind speed of 80 m/s.

The bending moments for the peak in both the x and y directions are shown in Figure 4.5, and their respective rotational displacement θ_x and θ_y in Figure 4.6. The maximum rotational displacement in the x direction reaches the value of 0.0036 radians, not enough to damage the blade structure, as it does not reach the minimum value to induce failure in the structure. Due to the turbulence pattern used in the aeroelastic tool the mean wind speed could not be increased anymore.

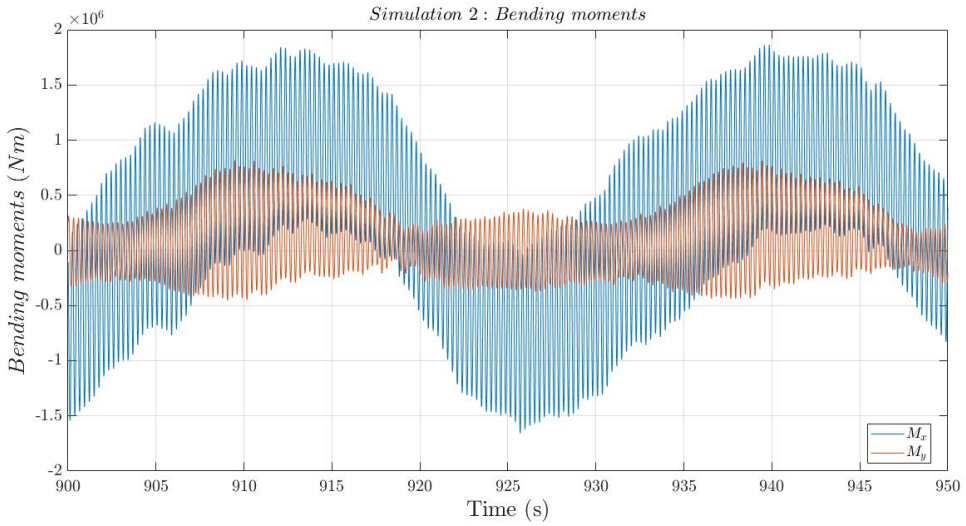

Figure 4.5: Case study 2. Cross-sectional bending moments in the peak zone of the new extreme wind profile.

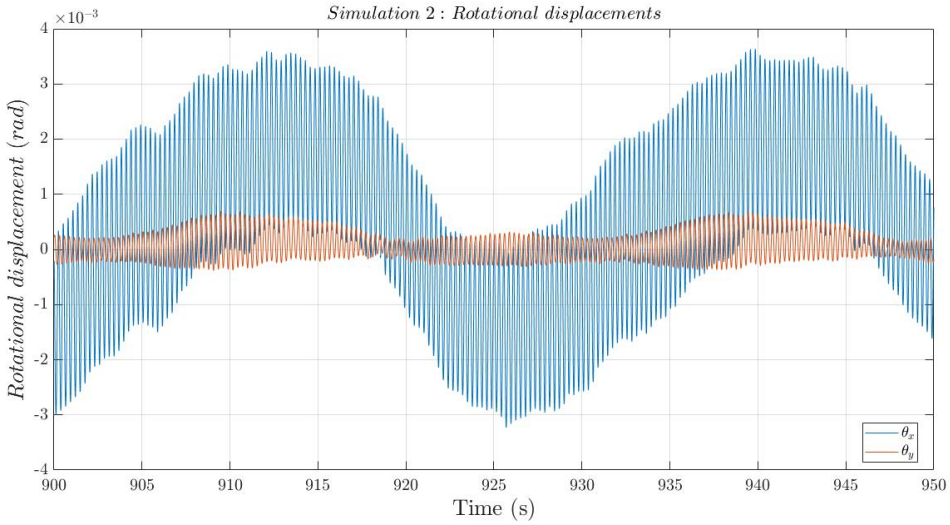

Figure 4.6: Case study 2. Rotational displacements corresponding to the bending moments in the peak zone of the new extreme wind profile.

Simulations in the 3D FE software were performed either way and, as expected thanks to the sensitivity study, no damage is induced in the blade structure with the new extreme wind profile. Delamination in the unidirectional composite material was also checked and Table 4.4 shows that no delamination occurred either. However, the strain values obtained in this simulation are higher than in Case study 1, as higher loads are applied with this new extreme wind profile.

Table 4.4: Case study 2. Check for delamination in the UD composite material.

UD composite material	ϵ_{33}	ϵ_{13}	ϵ_{23}
Ultimate strain	2.100e-03	1.100e-02	8.100e-03
Simulation max. strain	1.250-03	1.379e-03	4.576e-04

Although a new extreme wind profile was applied in this case study to induce damage in the blade section, results show that even in this extreme conditions the wind turbine can withstand the higher loads. Again, this is proof that the blade structure design is remarkable and the materials used can even resist the highest of the extreme loading conditions. It should be noted that the 3D modelled blade structure is assumed to be a perfect new blade that has not suffered from fatigue loads, and manufacturing flaws nor blade degradation are considered.

4.4 Change of foam core material

Given that the blade structure design can withstand both wind profiles from Case studies 1 and 2 respectively, a change in the foam core material of the sandwich structures will be studied to analyse how the blade structure will react under the previous wind conditions if having materials with different mechanical properties. Table 4.5 reflects the change of the foam core material properties from the ones used in the original blade structure.

Table 4.5: Change in the mechanical properties of foam core material.

Foam core material	Young's Modulus, E (MPa)	Yield strength, σ_y (MPa)
Original	30	0.5
Defective	10	0.1

4.4.1 Case study 3: Wind profile from Case study 1

When applying the modelled extreme wind profile from Case study 1 to the modified blade structure, still no damage is induced in the wind turbine blade structure. Although the mechanical properties of the foam core material are lower in this case, the extreme wind profile from Case study 1 is not extreme enough to produce failure in the blade section. Table 4.6 shows that no delamination occurs either in the unidirectional composite material.

Table 4.6: Case study 3. Check for delamination in the UD composite material.

UD composite material	ϵ_{33}	ϵ_{13}	ϵ_{23}
Ultimate strain	2.100e-03	1.100e-02	8.100e-03
Simulation max. strain	1.658-04	2.760e-04	8.291e-05

4.4.2 Case study 4: Wind profile from Case study 2

However, when applying the extreme wind profile from Case study 2, damage is induced in the blade structure, as the foam core in both the leading and the trailing panels experience plastic deformation, as shown in Figure 4.7. Since the blade structure has permanent damage, the stiffness properties need to be computed with the 3D FE software and updated into the aeroelastic tool.

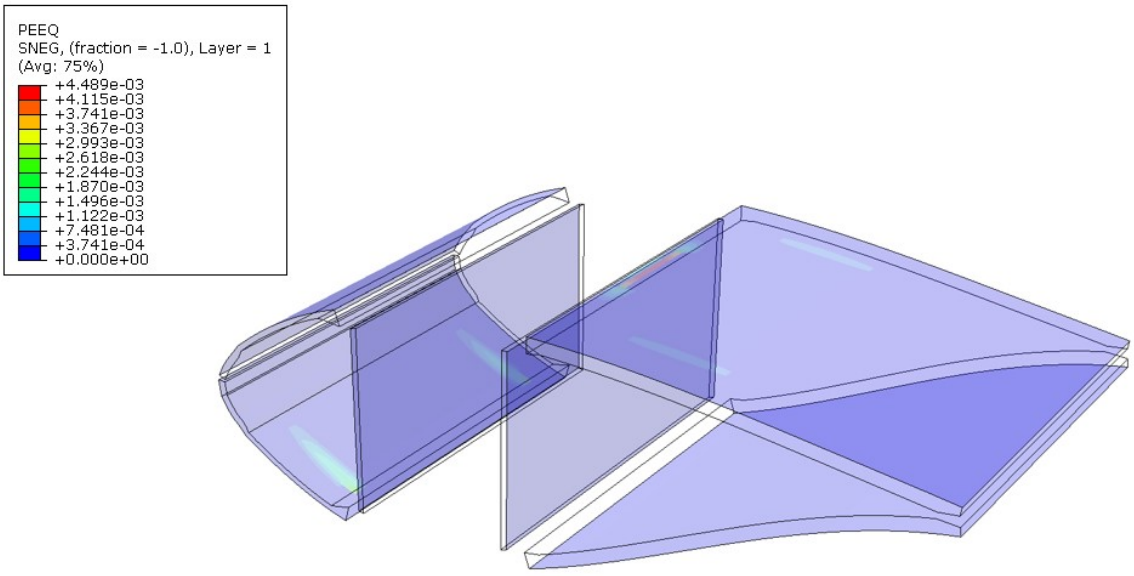

Figure 4.7: Case study 4. Plastic deformation in the foam core material of the blade structure.

Table 4.7 shows the percentage of degradation of the stiffness properties in this case study. As previously mentioned in Section 3.2.5, the update of stiffness properties is done with the stiffness matrix (equation 2.1). Each of the diagonal terms are computed with equations

3.10, 3.11, 3.12, 3.13, 3.14 and 3.15, and the elastic modulus E and shear modulus G can be obtained with the cross-sectional area of the blade section and the shear factors, as mentioned in Section 3.2.5.

Table 4.7: Case study 4. Degradation of the stiffness properties after damage induced in the blade structure.

Stiffness properties	**Before loading**	**After loading**	**% degradation**
E (GPa)	10.937	10.913	0.22%
G (GPa)	2.177	2.095	3.78%

Table 4.8 shows that no delamination of the UD material occurs in these circumstances. It makes sense, since the UD composite material has not been changed, just the foam core properties, and it makes sense that no delamination occurs in this case either.

Table 4.8: Case study 4. Check for delamination in the UD composite material.

UD composite material	ϵ_{33}	ϵ_{13}	ϵ_{23}
Ultimate strain	2.100e-03	1.100e-02	8.100e-03
Simulation max. strain	1.354-03	1.380e-03	4.867e-04

Although in this scenario damage is induced in the blade structure, it is important to remark that the modified foam core material has extremely low mechanical properties, which would not be realistic to have in a real-life scenario. These low mechanical properties in the foam core materials would only have sense in the case the material has pre-existing in-service damage. A extremely light foam is chosen to study the degradation of stiffness properties when damage is induced in the blade structure, and to analyse the significance of updating the stiffness properties when damage occurs, since the aerodynamic loads will be affected by this change in the structural properties.

5 Conclusions and future work

The purpose of this study is to couple an aeroelastic tool with a 3D FE software through an interface developed in MATLAB to study the possible degradation of wind turbine blade stiffness properties when damage is induced in the wind turbine blade structure. Under normal weather conditions there should be no induced damage in blade structures. However, their behaviour under extreme wind conditions is uncertain given that they are in an scenario that is outside of their design limits.

In this project, 3D blade model updating is done by coupling HAWC2 and ABAQUS, to account for structural non-linearities associated with geometry and composite layup that are neglected in the beam theory model used by the aeroelastic tool HAWC2. An interface that links the aeroelastic simulation of wind turbines and 3D FE modelling of blades has been developed using MATLAB. Using the HAWC2 software, the extreme wind profile is modelled, and the aerodynamic loads are calculated and used as boundary conditions of 3D FE modelling of blade sections. The structural stiffness predicted using the FEA software ABAQUS is inputted to HAWC2 to update the aerodynamic loads if damage is induced in the blade structure. Since both the aerodynamic loads and the structural properties of the blade influence each other, the behaviour of the blade can be predicted with 3D blade model updating.

A wind profile was modelled for this study fulfilling the characteristics of an extreme wind profile that can be found in adverse weather conditions. Real turbulence measurements were employed in the creation of this extreme wind profile to study how the DTU 10 MW Reference Wind Turbine will perform under extreme weather environments. The study showed that the blade structure for the mentioned wind turbine has great design specifications along with a good choice of materials, as it is capable to withstand extreme wind speeds. A perfect new blade structure was assumed, without considering fatigue loads, manufacturing flaws or blade degradation, and no damage was induced in the blade.

However, to test the performance of the developed interface, the foam core material in the blade structure was weakened, in order to induce damage in the blade structure and study the degradation of the stiffness properties. Under this scenario, degradation of the blade stiffness properties was found, and the interface correctly updated the results into the aeroelastic tool HAWC2. This way, a step has been moved towards the integrated design of wind turbines where both the aeroelastic and structural context of wind turbine blades are considered. Even though for these case studies the wind profile and the material had to be changed to induce damage in the blade structure, this has no impact in the interface's performance. This interface can work with infinite wind profile models and other blade structures belonging to other wind turbines, with different geometry and different material conditions.

The idea behind the development of this interface creates added value to the research community, as this interface helps in the wind turbine blade behaviour prediction under certain wind conditions. The interface can help in the decision process of repairing a

wind turbine blade before or after the upcoming of a storm. Future work to improve the interface's performance could include:

- Include a code to allow automatic blade failure analysis in the blade structure. Currently, after obtaining the stiffness properties the update can be done if there is damage induced in the blade, but the detection of foam core crush and delamination is checked manually by checking the 3D blade structure in ABAQUS.
- Build a Graphical User Interface (GUI) in MATLAB to make the interface more user-friendly.
- Consider a dynamic approach inside the aeroelastic tool HAWC2 to update the stiffness properties of blade structures automatically during the simulations.

Bibliography

[1] S. Chasing, "Crazy texas tornado bends wind turbine blades." Available online: https://www.youtube.com/watch?v=dRht4tkQJIM (accessed on February 12, 2023).

[2] K. Branner, J. Blasques, T. Kim, V. Fedorov, P. Berring, R. Bitsche, and C. Berggreen, "Anisotropic beam model for analysis and design of passive controlled wind turbine blades," 2012.

[3] T. U. of Denmark, "Modelling turbulence fields in hawc2." HAWC2 Selfstudy, Lecture notes, DTU Wind Energy, Technical University of Denmark, 2013.

[4] X. Chen and M. A. Eder, "Introduction to design of large composite structures." Desing of Large Composite Structures, Lecture notes, DTU Wind Energy, Technical University of Denmark, 2022.

[5] B. H. Jørgensen, P. H. Madsen, G. Giebel, I. Martí, K. Thomsen, and L. Assessment, "DTU international energy report 2021: Perspectives on wind energy," 2021.

[6] D. Hutchins, "The risks and opportunities of offshore wind energy." Available on: https://www.globalriskintel.com/insights/risks-and-opportunities-offshore-wind-energy#:~:text=Offshore%20wind%20farms%20face%20a,political%20considerations%2C%20and%20residential%20complaints. (accessed on February 15, 2023).

[7] X. Chen and J. Z. Xu, "Structural failure analysis of wind turbines impacted by super typhoon usagi," *Engineering failure analysis*, vol. 60, pp. 391–404, 2016.

[8] X. Chen, C. Li, and J. Xu, "Failure investigation on a coastal wind farm damaged by super typhoon: A forensic engineering study," *Journal of Wind Engineering and Industrial Aerodynamics*, vol. 147, pp. 132–142, 2015.

[9] D. Schroeder, "How do wind turbines survive severe storms?." Available online: https://www.energy.gov/eere/articles/how-do-wind-turbines-survive-severe-storms (accessed on February 12, 2023).

[10] R. P. Worsnop, J. K. Lundquist, G. H. Bryan, R. Damiani, and W. Musial, "Gusts and shear within hurricane eyewalls can exceed offshore wind turbine design standards," *Geophysical research letters*, vol. 44, no. 12, pp. 6413–6420, 2017.

[11] S. Rose, P. Jaramillo, M. J. Small, I. Grossmann, and J. Apt, "Quantifying the hurricane risk to offshore wind turbines," *Proceedings of the National Academy of Sciences*, vol. 109, no. 9, pp. 3247–3252, 2012.

[12] NREL, "Turbine models." Available online: https://github.com/NREL/turbine-models/blob/master/Offshore/DTU_10MW_178_RWT_v1.csv (accessed on February 27, 2023).

[13] C. Bak, F. Zahle, R. Bitsche, T. Kim, A. Yde, L. C. Henriksen, P. B. Andersen, A. Natarajan, and M. H. Hansen, "Design and performance of a 10mw wind turbine," *J. Wind Energy*, 2013.

[14] IEC 61400-3., "International electro technical committee iec 61400-3: Wind turbines part 3: Design requirements for offshore wind turbines.," *Edition1, Geneva*, 2009.

[15] G. Hagerman, "Tap-672-development of an integrated extreme wind, wave, current, and water level climatology to support standards-based design of offshore wind projects," 2013.

[16] I. Jeong, H. Kim, H. Cho, H. Park, and T. Kim, "Initial structural damage detection approach via fe-based data augmentation and class activation map," *Structural Health Monitoring*, p. 14759217221149612, 2023.

[17] X. Chen, S. Semenov, M. McGugan, S. H. Madsen, S. C. Yeniceli, P. Berring, and K. Branner, "Fatigue testing of a 14.3 m composite blade embedded with artificial defects–damage growth and structural health monitoring," *Composites Part A: Applied Science and Manufacturing*, vol. 140, p. 106189, 2021.

[18] T. J. Larsen, A. M. Hansen, and T. Buhl, "Aeroelastic effects of large blade deflections for wind turbines," *Proceedings of The Science of Making Torque from Wind*, pp. 238–246, 2004.

[19] B. B. Garzon, L. C. Henriksen, A. D. Hansen, N. A. Cutululis, and P. E. Sørensen, "Coupling of hawc2 and matlab: Towards an integrated simulation platform," in *2010 European Wind Energy Conference and Exhibition*, European Wind Energy Association (EWEA), 2010.

[20] D. Kaufer, N. Cosack, C. Böker, M. Seidel, and M. Kühn, "Integrated analysis of the dynamics of offshore wind turbines with arbitrary support structures," in *European Wind Energy Conference, Marseille, France*, Citeseer, 2009.

[21] G. Papazafeiropoulos, M. Muñiz-Calvente, and E. Martínez-Pañeda, "Abaqus2matlab: A suitable tool for finite element post-processing," *Advances in Engineering Software*, vol. 105, pp. 9–16, 2017.

[22] MATLAB, *MATLAB version 9.9.0 (R2020b)*. Natick, Massachusetts: The MathWorks Inc., 2021.

[23] M. A. Eder and X. Chen, "Fastigue: A computationally efficient approach for simulating discrete fatigue crack growth in large-scale structures," *Engineering Fracture Mechanics*, vol. 233, pp. 1–17, 2020.

[24] T. Larsen and A. Hansen, "How 2 hawc2, the user's manual," *User Manual, Risø National Laboratory*, 2021.

[25] T. U. of Denmark, "A servo-aeroelastic wind turbine simulation tool." HAWC2 Selfstudy, Lecture notes, DTU Wind Energy, Technical University of Denmark, 2013.

[26] J. Mann, "Wind field simulation," *Probabilistic Engineering Mechanics*, vol. 13, no. 4, pp. 269–282, 1998.

[27] T. U. of Denmark, "Large scale wind systems and local turbulence." HAWC2 Selfstudy, Lecture notes, DTU Wind Energy, Technical University of Denmark, 2013.

[28] T. U. of Denmark, "Aerodynamic model." HAWC2 Selfstudy, Lecture notes, DTU Wind Energy, Technical University of Denmark, 2013.

[29] T. U. of Denmark, "Structural model." HAWC2 Selfstudy, Lecture notes, DTU Wind Energy, Technical University of Denmark, 2013.

[30] R. D. Bitsche and J. P. Blasques, "Introduction to becas." HAWC2 Selfstudy, Lecture notes, DTU Wind Energy, Technical University of Denmark, 2013.

[31] R. D. Bitsche, "An introduction to beam cross section stiffness and mass properties." HAWC2 Selfstudy, Lecture notes, DTU Wind Energy, Technical University of Denmark, 2013.

[32] X.-Y. Miao and X. Chen, "Structural transverse cracking mechanisms of trailing edge regions in composite wind turbine blades," *Composite Structures*, vol. 308, pp. 116–680, 2023.

[33] N. H. Center and C. P. H. Center, "Saffir-simpson hurricane wind scale." Available on: `https://www.nhc.noaa.gov/aboutsshws.php` (accessed on February 27, 2023), 2022.

[34] T. U. of Denmark, "Database on wind characteristics." Available on: `https://gitlab.windenergy.dtu.dk/fair-data/winddata-revamp/winddata-documentation/-/blob/master/readme.md/` (accessed on October 24, 2022).

[35] K. S. Hansen, N. Vasiljevic, and S. A. Sørensen, "Turbulence measurements." Available on: `https://doi.org/10.11583/DTU.c.5405292.v14` (accessed on October 24, 2022).

[36] K. S. Hansen, N. Vasiljevic, and S. A. Sørensen, "Turbulence measurements from the skipheya masts.." Available on: `https://doi.org/10.11583/DTU.14380766.v1` (accessed on October 24, 2022).

[37] M. McWilliam, N. Bonfils, N. K. Dimitrov, and S. Dou, "Wind farm parameterization and turbulent wind box generation," *Hiperwind*, 2022.

[38] J. Mann, "The spatial structure of neutral atmospheric surface-layer turbulence," *Journal of Fluid Mechanics*, vol. 273, pp. 141−168, 1994.

[39] N. Dimitrov and A. Natarajan, "Application of simulated lidar scanning patterns to constrained gaussian turbulence fields for load validation," *Wind Energy*, vol. 20, no. 1, pp. 79–95, 2017.

[40] T. Carlinco, "Wind turbine on white background front view 3d image." Available on: `https://www.123rf.com/photo_3361701_wind-turbine-on-white-background-front-view-3d-image.html` (accessed on February 15, 2023).

[41] M. Smith, *ABAQUS/Standard User's Manual, Version 6.22*. United States: Dassault Systèmes Simulia Corp, 2022.

[42] D. W. Energy, "Vind abaqus cluster." Available on: `https://docs-devel.hpc.ait.dtu.dk/clusters/abaqus/readme/` (accessed on February 20, 2023).

[43] United Nations, "The Sustainable Development Agenda." Available on: `https://www.un.org/sustainabledevelopment/development-agenda/` (accessed on May 21, 2023).

[44] P. Bojek, "Renewable Electricity." Available on: `https://www.iea.org/reports/renewable-electricity` (accessed on May 27, 2023).

[45] IEA, "Global energy and climate model." IEA, Paris. License: CC BY 4.0. Available on: `https://www.iea.org/reports/renewable-electricity` (accessed on May 27, 2023), 2022.

[46] IRENA, "Wind energy." Available on: `https://www.irena.org/Energy-Transition/Technology/Wind-energy` (accessed on May 27, 2023), 2022.

A Sustainable Development Goals

The Sustainable Development Goals, also referred to as SDGs, are an appeal for everyone to preserve the environment, take action to eradicate poverty, and enhance the lives and futures of everyone in all parts of the world [43]. In total, there are 17 goals, which have been created to achieve a more sustainable and better world for all. In 2015, all the United Nation's Member States gathered together to develop the 2030 Agenda for Sustainable Development as part of a 15-year strategy to accomplish these 17 goals. However, at the current pace, not enough progress is being made in order to meet all goals by 2030.

The aim of this project is to contribute to the fight against climate change by developing new technologies to predict the behaviour of wind turbine blades under certain wind conditions and increase the overall service life of wind turbines. In particular, an interface has been developed to calculate more accurately the influence of the aerodynamic loads in the structural properties of wind turbine blades under extreme wind conditions. Under these circumstances, damage can be induced in the blade structure, and the structural damage in wind turbine blades affects the aerodynamic loads.

There are three main sustainable development goals directly related to this study, sorted by relevance, as can be seen in Figure A.1:

- **Goal 7:** Affordable and Clean Energy.
- **Goal 13:** Climate Action.
- **Goal 9:** Industries, Innovation, and Infrastructure.

Figure A.1: Sustainable Development Goals related to this study.

The first SDG related to this study is goal no. 7: Affordable and Clean Energy. The main concern of this goal is to ensure everyone has access to inexpensive, renewable energy. Renewable energies are essential to clean energy transitions. According to early projections, 2022 will be a record year for renewable energy capacity expansion, with an annual capacity of roughly 340 GW expected to rise [44]. The world is moving closer to its sustainable energy goals. But at the current rate of development, Goal 7 will not be accomplished by 2030.

It is important to continue investing in the use of renewable energy resources, as producing energy primarily from fossil fuels like coal, oil, or gas results in the emission of significant volumes of greenhouse gases that have a negative impact on both human health and the environment. With this project, the production of renewable energy is promoted through research into new technologies that favour the production of wind energy, seeking to increase the useful life of wind turbines.

Another goal directly related to this project is goal no. 13: Climate Action. With the glaciers melting and the sea level rising, the global temperature has already increased by 1.1° C over pre-industrial levels. Flooding and drought are further effects of climate change that cause millions of people to be ripped away, losing access to essential services like health and education, slowing economic progress, and spreading and widening inequality. Therefore, it is crucial to act quickly to prevent climate change and its catastrophic effects in order to save lives and livelihoods. It is also essential to achieving the 17 Goals of the 2030 Agenda for Sustainable Development, which are the road map for a brighter future [43].

The implementation of renewable energies is one of the primary factors in fighting against climate change by limiting the increase in the world average temperature below 1.5° C [44]. However, the growth of renewable power must be more rapid to meet the targets under the Net Zero Emissions by 2050 Scenario, where the renewable share of generation rises from just under 29% in 2021 to more than 60% by 2030. The Net Zero Emissions by 2050 Scenario (NZE) is an established International Energy Agency (IEA) scenario that outlines a route for the world's energy sector to attain net zero CO2 emissions by 2050, with industrialized economies achieving net zero emissions ahead of others [45]. This scenario satisfies important energy-related Sustainable Development Goals by reaching universal access to energy by 2030, directly related to the previously mentioned goal no. 7. To meet the Net Zero Scenario, renewable electricity generation has to keep growing by more than 12% annually throughout the years 2022 - 2030. Despite unprecedented increases in renewable capacity, power growth fell well short of the Net Zero Scenario milestone in 2021. All renewable technologies will need to be installed much more quickly around the globe in order to meet the planned targets.

The last goal related to this study is goal no. 9: Industry, Innovation and Infrastructure. Goal 9 aims to create innovative environments, advance sustainable industry, and create resilient infrastructure. Infrastructure investing, sustainable industrial development, and innovations in technology all play a significant role in economic expansion, social progress, and climate action.

With the interface developed in this study, there is a contribution in the development of new technologies that make renewable energy, in particular wind energy, more accessible to the world. This interface allows to perform simulations to predict the behaviour of wind turbine blades under certain wind conditions. In addition, it is able to predict more accurately their behaviour under extreme wind conditions where the developed interface plays a key role, as it has been specially designed to take into account extreme wind scenarios to predict if wind turbine blades will survive the effects of a storm or tornado. Figure A.2 shows an overview of the interface's workflow, where the wind turbine is modelled in the aeroelastic tool HAWC2 to calculate the aerodynamic loads that will be transferred to the 3D wind turbine blade model and see if damage is induced under extreme wind conditions.

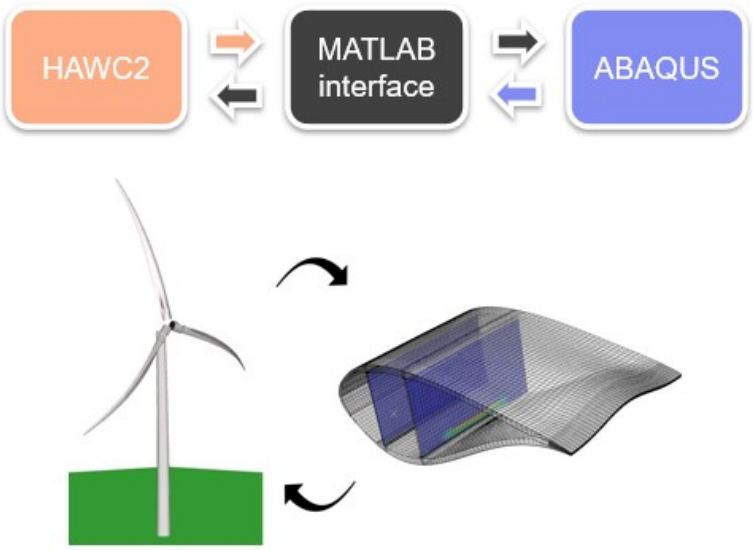

Figure A.2: Interface's key role: Wind turbine blade behaviour prediction.

As wind turbines are exposed to external conditions it is inevitable that their performance will deteriorate over time. And when subject to extreme wind conditions, damage can be induced in wind turbine blades that, if not replaced on time, it could potentially damage the whole wind turbine structure. The developed interface helps to predict how wind turbine blades are going to behave, and can help in the decision process whether blades should be repaired or replaced before or after extreme wind conditions. This interface optimizes the wind power production by choosing which wind turbines should be in operation and which ones should be repaired.

Table A.1 shows all the SDGs related to the project with its respective dimension, role, and goal.

Table A.1: Description of the Sustainable Development Goals related to this study.

SDG dimension	SDG identified	Role	Goal
Society	Goal no. 7: Affordable and Clean Energy	Primary	"By 2030, enhance international cooperation to facilitate access to clean energy research and technology, including renewable energy, energy efficiency and advanced and cleaner fossil-fuel technology, and promote investment in energy infrastructure and clean energy technology."
Biosphere	Goal no. 13: Climate Action	Primary	"Strengthen resilience and adaptive capacity to climate-related hazards and natural disasters in all countries."
Economic	Goal no. 9: Industries, Innovation, and Infrastructure	Secondary	"By 2030, upgrade infrastructure and retrofit industries to make them sustainable, with increased resource-used efficiency and greater adoption of clean and environmentally sound technologies and industrial processes, with all countries taking action in accordance with their respective capabilities."

A.1 Quantification of the impact of the contribution to the SDGs

New technologies are being used to transform the wind energy sector. The interface developed in this study is a pioneer version of a digital twin, which is a digital representation of an actual item (in this case a wind turbine) used to replicate its behavior under various circumstances. Sensors collect real life data measurements that can be monitored to make simulations and more accurately estimate the useful life of wind turbines and predict how many will be needed in a certain wind farm over time. Since 2000, wind power has expanded quickly thanks to R&D, supporting laws, and declining costs. According to IRENA's data (International Renewable Energy Agency), the installed wind production capacity worldwide has expanded by a factor of 98 over the previous 20 years, rising from 7.5 GW in 1997 to about 733 GW by 2018.

While offshore wind capacity increased proportionately faster, but from a smaller base, from 3.1 GW in 2010 to 34.4 GW in 2020, onshore wind capacity increased from 178 GW in 2010 to 699 GW in the same period, as summarized in Table A.2. Between 2009 and 2019, the amount of wind energy produced rose by a factor of 5.2, reaching 1412 TWh [46].

Table A.2: Evolution of the wind capacity worldwide from 2010 to 2020.

Wind capacity worldwide	Onshore (GW)	Offshore (GW)
2010	178	3.1
2020	699	34.4

Costs have decreased and capacity factors have grown as technology has evolved and scaled up. The global weighted-average levelized cost of electricity (LCOE) for onshore wind decreased from USD 0.089/kWh to USD 0.039/kWh between 2010 and 2020, a 56% decrease (Figure A.3). The LCOE of newly launched offshore wind projects decreased by about half (48%) throughout the same time frame.

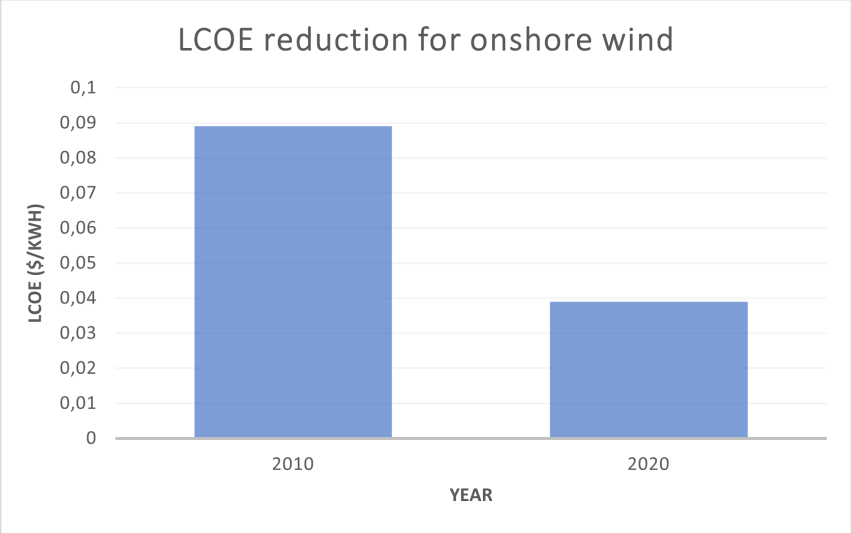

Figure A.3: LCOE reduction for onshore wind.

The size of the turbine and the length of its blades determine how much electricity can be generated. The output is inversely related to the rotor's size and to the square of the wind speed. The wind power potential theoretically increases by a factor of eight when wind

speed doubles. The capacity of wind turbines has grown over time. In 1985, conventional turbines had rotor diameters of 15 meters and rated capacities of 0.05 MW. The capacity of the turbines in today's new wind power projects ranges from 3 to 4 MW onshore and 8 to 12 MW offshore [46].

Table A.3: Evolution of the rated capacity of wind turbines.

Rated capacity	Onshore (MW)	Offshore (MW)
1985	0.05	-
2020	3-4	8-12

To improve renewable energy, several intergovernmental and commercial collaborative programs are in operation. For the European Union's 2030 renewable energy goals and in response to the energy crisis brought on by Russia's invasion of Ukraine, several European nations have already increased the scope of their renewable support programs and are working to accelerate the spread of renewable energy all across the world.

B Appendix: Pseudocodes

Algorithm 1 main.m

1: Initialisation: Define the number of iterations of the whole simulation, the time of the unloading step, and indicate if the Mz moment is going to be neglected.
2: **for** The number of iterations **do**
3: Check working folder.
4: Simulation setup: name of the .htc file, .dat file, .inp file and wind profile file (each iteration has its own files).
5: Call the function `readwindprofile` to obtain the .bin turbulence files.
6: Run HAWC2.
7: Obtain HAWC2 outputs: Open .sel file, read, and store results.
8: Call the function `convert_mom2ang` to convert the cross-sectional moments M_x and M_y into rotational displacements θ_x and θ_y.
9: Save θ_x and θ_y as .inp files (loading input files for ABAQUS).
10: Call the function `inp2m` to create the function that will create the .inp file with HAWC2 loading.
11: Call the function `inp_initial_v8` to create the ABAQUS input .inp file.
12: Call ABAQUS to run the simulation.
13: Call function `Read_ODB_outputs_node` to read the ABAQUS results.
14: Compute stiffness properties: call ABAQUS to run the .inp files to compute the stiffness properties.
15: Call the function `obtain_stiffness_prop` to obtain the stiffness properties.
16: **if** damage induced in blade section **then**
17: Call the function `update_HAWC2` to update the new stiffness properties in HAWC2.
18: **end if**
19: Plot results
20: **end for**

Algorithm 2 readwindprofile.m

```
Open the folder where the turbulence measurements are.
Open the wind profile file in read mode and save the results in fidw.
Scan the text and save it in variable Cw.
Get the number of lines in Cw.
Initialise dummy variables for the forloop.
for the number of lines in Cw do
    Search for the header section of the file.
    Search for the sensor statistics section of the file.
    Search for the data field section of the file.
    if reached header section then
        Search for the duration of the wind profile.
        Search for the frequency of the samples.
        if reached duration then
            Save the value of the duration of the data measurements in variable total_time_w.
        end if
        if reached frequency then
            Save the value of the frequency of the samples in variable freq.
        end if
    end if
    if reached sensor statistics section then
        Dummy variable count_sensor to count how many times it gets inside the if statement.
        The sensor measures where wsp is max is defined before.
        if count sensor == position where wsp is max then
            Get the information of that sensor measurements and save it in the following variables sensor_height, wsp, std_num, max_wind_speed, and tint.
        end if
    end if
    if reached data field section then
        Save the data field corresponding to the selected sensor measures.
    end if
    If statements to change between sections.
end for
Substract the mean wind speed wsp from the data measurements to get the turbulence measurements.
Write them in a .dat file so that HiperSim can read the turbulence measurements from the turbulence file.
Plot the wind profile
Close the file.
Go back to the MATLAB folder.
```

Algorithm 3 function [*sig*, Freq, Time, Flag, Binary] = ReadHawc2(FileName)

Open FileName (.sel file) in read mode and save the status in fid variable
if fid == -1 **then**
    Variable $Flag = 0$
    Display warning message that the file could not be found
    sig matrix = [], variable $Freq = 0$, variable $Time = 0$, variable $Binary = 0$
end if
Skip first 8 lines of .sel file (useless information)
Read line number 9 and store the values for number of scans N, number of channels Nch, time $Time$, and file format $FileType$
Close file
Calculate the sampling frequency $Freq$ as $N/Time$
Store the time of the simulation manually as $t = [1/\text{Freq}: 1/\text{Freq}:\text{Time}]'$
if file format == BINARY **then**
    Set $Binary = 1$
    Open .dat file in read mode and save the status in fid variable
    Store values in matrix *sig*
    if *sig* is empty **then**
        Variable $Flag = 0$
        Display warning message that there is no data in .dat file
        sig matrix = [], variable $Freq = 0$, variable $Time = 0$, variable $Binary = 0$
        Return
    end if
    Read scale factor from the .sel file
    Update *sig* by multiplying it by the scale factor
    Close file
    Variable $Flag = 1$
else if file format == ASCII **then**
    Set $Binary = 0$
    Read the .dat file and save the status in *sig* variable
    Store values in matrix *sig*
    if *sig* is empty **then**
        Variable $Flag = 0$
        Display warning message that there is no data in .dat file
        sig matrix = [], variable $Freq = 0$, variable $Time = 0$, variable $Binary = 0$
        Return
    end if
    if first column of *sig* matrix is lower than the number of scans N **then**
        Variable $Time$ computed as $Time = length(sig(:, 1))/Freq$
        Variable $Flag = 2$
        Display warning message that there is not full data in .dat file
        Return
    end if
    Variable $Flag = 1$
else
    Display warning message that it is an unknown file type
    Variable $Flag = 0$
end if
Asign the simulation time t to the first column of the matrix *sig*

Algorithm 4 function [theta_x, theta_y] = convert_mom2ang(blade_sec_data, L_sec, Mx_HAWC2, My_HAWC2)

blade_sec_data is a vector with the cross-section properties defined in Table 2.1.
L_sec is the value of the length of the blade section (1 m).
Mx_HAWC2 and My_HAWC2 are the cross-sectional moments obtained after running HAWC2.
Compute $k11$, $k22$, $k33$, $k44$, $k55$, and $k66$, the diagonal terms of the stiffness matrix defined in equation 2.1.
for the length of the cross-sectional moments vector **do**
    if Mx_HAWC2 is negative **then**
        Parameter $neg\_x = 1$
    else
        Parameter $neg\_x = 0$
    end if
    if My_HAWC2 is negative **then**
        Parameter $neg\_y = 1$
    else
        Parameter $neg\_y = 0$
    end if
    Calculate the curvature κ using equation 3.5 for both the x and y direction.
    Calculate the radius of curvature using equation 3.6 for both the x and y direction.
    Calculate the angle β using the equation 3.7 for both the x and y direction.
    Calculate the displacement δ using equation 3.8 for both the x and y direction.
    Calculate the rotational displacement theta_x and theta_y using equation 3.9.
    Assign the correct sign to the rotational displacement angle.
    if neg_x == 1 **then**
        theta_x has negative sign.
    end if
    if neg_y == 1 **then**
        theta_y has negative sign.
    end if
end for

Algorithm 5 inp2m.m

1: Check working folder.
2: Write the constructor .m file to create a function in a MATLAB script that will generate the .inp ABAQUS file, as $OutputFileName = inp\_initial.m$.
3: Open a new file for writing in text mode and save the status in $fileID$ variable.
4: Print the name of the function and the input variables, which are the name of the .inp ABAQUS file, and the rotational displacements theta_x and theta_y stored in .inp files.
5: Print the name of the .inp file.
6: Print the command to open the .inp file for writting in text mode.
7: Open the current .inp ABAQUS file and scan the text.
8: Indicate the number of amplitudes that there will be in the .inp file and its respective angles.
9: Initialise dummy variables for the $forloop$.
10: **for** the number of lines in the .inp file **do**
11: Search for the amplitude zone. When reached, variable *amplitude* will not be 0.
12: Search for the loads zone. When reached, variable *load* will not be 0.
13: Search for the dynamic step zone. When reached, variable *time_dyn* will not be 0.
14: Search for the static step zone. When reached, variable *time_st* will not be 0.
15: Search for the node output zone. When reached, variable *reach_output* will not be 0.
16: Search for the node print zone. When reached, variable *reach_print* will not be 0.
17: **if** reached amplitude zone **then**
18: Count the number of times it gets inside the if statement.
19: Variable C_{line} stores information regarding the amplitude name and its respective angle.
20: **if** finished reading amplitude lines **then**
21: Reset the count.
22: **end if**
23: **end if**
24: **if** reached load zone **then**
25: Count the number of times it gets inside the if statement.
26: Variable C_{line} stores information regarding the load name in ABAQUS and its respective amplitude name.
27: **if** finished reading load lines **then**
28: Reset the count.
29: **end if**
30: **end if**
31: **if** reached dynamic step zone, dummy variable $dynamic == 1$ **then**
32: Variable C_{line} stores information regarding the time increment, the duration of the step, the minimum and the maximum time increment.
33: Set dummy variable $dynamic = 0$.
34: **end if**
35: **if** reached static step zone, dummy variable $static == 1$ **then**
36: Variable C_{line} stores information regarding the time increment, the duration of the step, the minimum and the maximum time increment.
37: Set dummy variable $static = 0$
38: **end if**
39: [...]
40: **end for**

Algorithm 6 inp2m.m: Continuation

for the number of lines in the .inp file **do**
    [...]
    if reached output or print zone, dummy variable *output* == 1 or *print* == 1 **then**
        Variable C_{line} stores information regarding the ABAQUS variables desired as outputs.
        Set dummy variable *output* and *print* = 0.
    end if
    Print variable C_{line}.
    if reached dynamic step zone **then**
        Dummy variable *dynamic* = 1 to indicate that the next line in the file is going to be modified.
    end if
    if reached static step zone **then**
        Dummy variable *static* = 1 to indicate that the next line in the file is going to be modified.
    end if
    if reached output step zone **then**
        Dummy variable *output* = 1 to indicate that the next line in the file is going to be modified.
    end if
    if reached print step zone **then**
        Dummy variable *print* = 1 to indicate that the next line in the file is going to be modified.
    end if
end for

Algorithm 7 [t_abq, Mx_abq, My_abq, Mz_abq, UR1_abq, UR2_abq, UR3_abq] = function Read_odb_outputs_node(name_dat_file, name_sta_file)

name_dat_file and name_sta_file are outputs file from ABAQUS.
while exist(name_dat_file, 'file') == 0 **do**
    Pause the code if the .dat file (ABAQUS output file) does not exist.
end while
Open $name\_dat\_file$ and save the status in $fidd$ variable.
Initialise dummy variable ii, to count the number of lines.
Initialise dummy variable jj, to store the results in the function output variables.
while the end of the file indicator is not reached **do**
    Store the text in the current line $tline$, and $ii = ii + 1$.
    if tline == 'NODE OUTPUT' **then**
        Count the number of steps.
        Read the next line and $ii = ii + 1$. ▷ This is done to skip the lines until the results part is reached.
        while tline has no numbers **do**
            Read the next line.
            Find the phrase 'ALL THE VALUES IN THIS TABLE ARE ZERO'.
            if phrase found **then**
                $jj = jj + 1$;
                Save output variables Mx_abq(jj), My_abq(jj), Mz_abq(jj), UR1_abq(jj), UR2_abq(jj), UR3_abq(jj) as zeros.
            end if
            $ii = ii + 1$;
        end while
        while tline has numbers **do**
            $jj = jj + 1$;
            Scan $tline$ and save it in $data\_f$.
            Save output variables Mx_abq(jj), My_abq(jj), Mz_abq(jj), UR1_abq(jj), UR2_abq(jj), UR3_abq(jj).
            Read the next line so it gets out of the while loop and $ii = ii + 1$.
        end while
    end if
end while
Open $name\_sta\_file$ and save the status in fid_sta variable.
Scan the text and save it in variable C_sta. ▷ Read the total time of the ABAQUS simulation from the .sta file.
Initialise dummy variables $exit$ and rr.
while exit == 0 **do**
    Count $rr = rr + 1$.
    Detect if the time step has the letter U (when there are convergence issues, several number of iterations can be done in a same time step. The iterations appear as '1U', '2U',...).
    if no letter **then**
        Continue the while loop
    end if
    for number of iterations with letter **do**
        if letter **then**
            Delete that row.
        end if
    end for
end while
If there are 2 steps in the ABAQUS job, store each time to its respective step.

Algorithm 8 [D_sim1, D_sim2, D_sim3, phi_sim1, phi_sim2, phi_sim3] = function Read_odb_outputs_node_stiffness_prop(name_dat_file)

```
name_dat_file is the output file from ABAQUS.
while exist(name_dat_file, 'file') == 0 do
    Pause the code if the .dat file (ABAQUS output file) does not exist.
end while
Open name_dat_file and save the status in fidd variable.
Initialise dummy variable i, to count the number of lines.
Initialise dummy variable j, to store the results in the function output variables.
while the end of the file indicator is not reached do
    Store the text in the current line tline, and i = i + 1.
    if tline == 'NODE OUTPUT' then
        Count the number of steps.
        Read the next line and i = i + 1.      ▷ This is done to skip the lines until the results part is reached.
        Erase the lines.
        while tline has no numbers do
            Read the next line and i = i + 1.
            Erase the lines.
            ii = ii + 1;
        end while
        while tline has numbers do
            j = j + 1;
            Scan tline and save it in data_f.
            Save output variables D_sim1(j), D_sim2(j), D_sim3(j),
                phi_sim1(j), phi_sim2(j), phi_sim3(j).
            Read the next line so it gets out of the while loop and i = i + 1.
        end while
    end if
end while
Close file.
```

Algorithm 9 [up_stiff_prop] = function update_stiffness_prop(name_axial_dat_file, name_sh_x_dat_file, name_sh_y_dat_file, name_bend_x_dat_file, name_bend_y_dat_file, name_torsion_dat_file)

1: Define the lenght of the blade section L_sec.
2: Define the loads applied in each direction: $Fx\_applied$, $Fy\_applied$, $Fz\_applied$, $Mx\_applied$, $My\_applied$, $Mz\_applied$.
3: State the paths of the .dat files.
4: Read .dat files.
5: For the six files, the displacements and rotational displacement in the 3 directions (x, y, z) will be obtained to calculate the strains and curvatures. With the stiffness matrix in equation 2.1 the diagonal terms of the matrix will be computed.
6: Call the function [ua_x, ua_y, ua_z, phia_x, phia_y, phia_z] = `Read_ODB_outputs_node_stiffness_prop`(axial_dat_path). ▷ Axial file: Fz.
7: Compute strains and curvatures: ea_x, ea_y, ea_z, ka_x, ka_y, ka_z.
8: Compute EA as $Fz\_applied/ea\_z$.
9: Call the function [ubx_x, ubx_y, ubx_z, phibx_x, phibx_y, phibx_z] = `Read_ODB_outputs_node_stiffness_prop`(bend_x_dat_path). ▷ Bending moment x direction file: Mx.
10: Compute strains and curvatures: ebx_x, ebx_y, ebx_z, kbx_x, kbx_y, kbx_z.
11: Compute EI_x as $Mx\_applied/kbx\_x$.
12: Call the function [uby_x, uby_y, uby_z, phiby_x, phiby_y, phiby_z] = `Read_ODB_outputs_node_stiffness_prop`(bend_y_dat_path). ▷ Bending moment y direction file: My.
13: Compute strains and curvatures: eby_x, eby_y, eby_z, kby_x, kby_y, kby_z.
14: Compute EI_y as $My\_applied/kby\_y$.
15: Call the function [ut_x, ut_y, ut_z, phit_x, phit_y, phit_z] = `Read_ODB_outputs_node_stiffness_prop`(torsion_dat_path). ▷ Torsion moment file: Mz.
16: Compute strains and curvatures: et_x, et_y, et_z, kt_x, kt_y, kt_z.
17: Compute GJ as $Mz\_applied/kt\_z$.
18: Call the function [usx_x, usx_y, usx_z, phisx_x, phisx_y, phisx_z] = `Read_ODB_outputs_node_stiffness_prop`(sh_x_dat_path). ▷ Shear force x direction file: Fx.
19: Compute strains and curvatures: esx_x, esx_y, esx_z, ksx_x, ksx_y, ksx_z.
20: Compute GAk_x as $Fx\_applied/esx\_x$.
21: Call the function [usy_x, usy_y, usy_z, phisy_x, phisy_y, phisy_z] = `Read_ODB_outputs_node_stiffness_prop`(sh_y_dat_path). ▷ Shear force y direction file: Fy.
22: Compute strains and curvatures: esy_x, esy_y, esy_z, ksy_x, ksy_y, ksy_z.
23: Compute GAk_y as $Fy\_applied/esy\_x$.
24: Write the equations of the stiffness matrix: forces = stiffness matrix · strains and curvatures.
25: Solve the system of equations to obtain the components of the stiffness matrix.
26: Knowing the area of the blade section, and component k33, the elastic modulus E is obtained.
27: Knowing k44 and k55, Ix and Iy are obtained.
28: The shear modulus G is obtained with either k11 or k22.
29: The torsional moment of inertia J is obtained dividing k66/G.
30: The vector up_stiff_prop stores the values of E and G.

Algorithm 10 function [blade_sec_data, blade_st_data] = Read_blade_st(blade_st_file, r_blade)

blade_st_file indicates the path to the .dat file that stores the cross-sectional properties of the blade sections.
r_blade indicates the section that is modelled in ABAQUS.
Open *blade_st_file* in read mode and save the status in $fidb$ variable.
Scan the text and save it in variable *Cb*.
Get the number of lines in *Cb*.
Save line number 4 in *Cb* into the variable *blade_st_data*, which stores the information of the columns in *Cb*.
for the number of lines in *Cb* **do**
    Search for the information for the blade section indicated in *r_blade*.
    if reached blade section **then**
        Save the cross-sectional properties in *blade_sec_data*.
    end if
end for
Close file.

Algorithm 11 function [blade_sec_data_updated, blade_st_data] = update_HAWC2(up_stiff_prop, name_updated_blade_st_file, name_blade_st_file, blade_st_file, r_blade, name_updated_htc_file, name_htc_file)

Open *blade_st_file* in read mode and save the status in $fidu$ variable.
Scan the text and save it in variable *Cb*.
Get the number of lines in *Cb*.
Initialise dummy variable *done*.
for the number of lines in *Cb* **do**
    Search for the information for the blade section indicated in *r_blade*.
    if reached blade section **then**
        Update the stiffness properties in *Cb* with the values in *up_stiff_prop*.
    end if
end for
Close file.